TITLE: Gas5 regulates early life stress-induced anxiety and spatial memory

Dipanjana Banerjee, Sania Sultana and Sourav Banerjee

National Brain Research Centre, NH – 8, Nainwal Mode, Manesar 122052, Haryana, India

Correspondence: souravnbrc@gmail.com or sourav@nbrc.ac.in

Keywords: Maternal separation, stress, long non-coding RNA, synapse, anxiety, spatial memory.

Abbreviations

- ***Ago***: *Argonaute*
- ***AAV***: *Adeno-Associated Virus*
- ***AMPA***: *α-Amino-3-hydroxy-5-methyl-4-isoxazolepropionic acid*
- ***ANOVA***: *Analysis of Variance*
- ***BCA***: *Bicinchoninic Acid*
- ***BSA***: *Bovine Serum Albumin*
- ***CA1***: *Cornu Ammonis 1*
- ***CA2***: *Cornu Ammonis 2*
- ***CA3***: *Cornu Ammonis 3*
- ***CIRTs***: *CRISPR-Cas-inspired RNA targeting systems*
- ***CD1***: *Outbred Swiss mice*
- ***CLIP-seq***: *Cross-Linking Immunoprecipitation followed by high-throughput sequencing*
- ***CMV***: *Cytomegalovirus*
- ***CPCSEA***: *Committee for the Purpose of Control and Supervision of Experiments on Animals*
- ***CRISPR***: *Clustered Regularly Interspaced Short Palindromic Repeats*
- ***cDNA***: *Complementary DNA*
- ***DH5α***: *Escherichia coli strain*
- ***DI***: *Discrimination Index*
- ***DMEM***: *Dulbecco's Modified Eagle Medium*
- ***DIV***: *Days In Vitro*
- ***DNA***: *Deoxyribonucleic Acid*
- ***dF***: *Degrees of Freedom*
- ***ECL***: *Enhanced Chemiluminescence*
- ***EDTA***: *Ethylenediaminetetraacetic Acid*
- ***EF1-α***: *Elongation Factor 1-alpha*
- ***EGFP***: *Enhanced Green Fluorescent Protein*
- ***ES***: *Early life stress*
- ***FBS***: *Fetal Bovine Serum*
- ***FDR***: *False Discovery Rate*
- ***Gas5***: *Growth Arrest Specific-5*
- ***GFP***: *Green Fluorescent Protein*
- ***GABAergic***: *Gamma-Aminobutyric Acidergic*

- ***GO***: *Gene Ontology*
- ***HEK293T***: *Human Embryonic Kidney 293 Cells, expressing large T antigen of SV40*
- ***HC***: *Homecaged*
- ***IAEC***: *Institutional Animal Ethics Committee*
- ***LSD***: *Least Significant Difference*
- ***MOI***: *Multiplicity of Infection*
- ***MRI***: *Magnetic Resonance Imaging*
- ***MS***: *Maternal separation*
- ***NcA***: *Nucleus accumbens*
- ***NEB***: *New England Biolabs*
- ***NMDA***: *N-Methyl-D-Aspartate*
- ***PBS***: *Phosphate Buffered Saline*
- ***PCR***: *Polymerase Chain Reaction*
- ***PFA***: *Paraformaldehyde*
- ***P***: *Postnatal Day*
- ***POSTAR3***: *Post-transcriptional Regulation Atlas of lncRNAs and mRNAs*
- ***Pvt1***: *Plasmacytoma Variant Translocation 1*
- ***qPCR***: *Quantitative Polymerase Chain Reaction*
- ***RBPs***: *Ribosome Binding Proteins*
- ***qRT-PCR***: *Quantitative Reverse Transcription Polymerase Chain Reaction*
- ***RISC***: *RNA-Induced Silencing Complex*
- ***Rmst1***: *rhabdomyosarcoma 2-associated transcript 1*
- ***RNAs***: *Ribonucleic acids*
- ***RNP***: *Ribonucleoprotein*
- ***SDS***: *Sodium Dodecyl Sulfate*
- ***SEM***: *Standard Error of the Mean*
- ***shRNAs***: *Short hairpin RNAs*
- ***Snhg8***: *Small Nucleolar RNA Host Gene 8*
- ***Snhg12***: *Small Nucleolar RNA Host Gene 12*
- ***SV40***: *Simian Virus 40*
- ***SynLAMP***: *Synaptic Lysosome-associated Membrane Protein*
- ***Tubulinβ-1***: *Beta-1 tubulin*
- ***UC***: *Universal Control*
- ***Zfas1***: *Zinc finger antisense 1*
- ***ZsGreen***: *Zoanthus sp. Green Fluorescent Protein*

ABSTRACT:

Early life stress (ES) induced by maternal separation (MS) remains a proven causality of anxiety and memory deficits at later stages of life. Emerging studies have shown that MS-induced gene expression in the hippocampus is operated at the level of transcription. However, the extent of involvement of non-coding RNAs in MS-induced behavioural deficits remains unexplored. Here, we have investigated the role of synapse-enriched long non-coding RNAs (lncRNAs) in anxiety and memory upon MS. We observed that MS led to an enhancement of expression of the lncRNA Gas5 (Growth Arrest Specific-5) in the hippocampus; accompanied by increased levels of anxiety and deficits in spatial memory. Gas5 knockdown in early life was able to reduce anxiety and partially rescue the spatial memory deficits of maternally separated adult mice. However, the reversal of MS-induced anxiety and memory deficits is not attributed to Gas5 activity during neuronal development as Gas5 RNAi did not influence spine development. Gene Ontology analysis revealed that Gas5 exerts its function by regulating RNA metabolism and translation. Our study highlights the importance of MS-regulated lncRNA in anxiety and spatial memory.

INTRODUCTION

Maternal separation, a well-established model of early-life stress, has been extensively studied to investigate the long-term consequences of adverse early life events during this critical period of brain function and behaviour (Taylor et al., 2010; Korosi et al., 2012). Stress due to maternal separation (MS) in rodents leads to anxiety-like behaviours in adulthood as characterized by heightened fear, avoidance, and stress sensitivity (Banqueri et al., 2017; Lundberg et al., 2020; Balouek *et al.*, 2023). The ventral hippocampus, a key brain area affected by MS (Dimatelis et al., 2014; Marais et al., 2009), has been shown to regulate emotions (Jimenez et al., 2018; H. Li et al., 2022; McNaughton, 1997). MS-induced anxiety can lead to changes in the total volume of the hippocampus (Kalisch et al. 2006) and alterations in the expression of glutamatergic receptors (Pickering et al. 2006), both NMDA (Barkus et al. 2010) and AMPA (Katsouli et al. 2014); GABAergic receptors (Sterley, Howells, and Russell 2013), and serotonergic as well as cholinergic receptors (File et al., 2000). Moreover, early-life stress can impact spatial memory that involves the dorsal hippocampus

129 (Morris *et al.*, 2006; Blum *et al.*, 1999). Such behavioural deficits are linked with
130 structural and functional modifications in the hippocampus (Izquierdo and Medina,
131 1997; Revest *et al.*, 2009; Kremmyda *et al.*, 2016). These observations indicate that
132 the enduring effects of maternal separation on anxiety and memory involve alterations
133 in synaptic plasticity (Monroy et al., 2010; Bannerman *et al.*, 2014) and
134 neurotransmitters, for example, noradrenaline and serotonin (Daniels et al. 2004).

135 More recently, transcriptomics analysis following MS identified a distinct set of miRNAs
136 in specific brain areas including the hippocampus (Mckibben and Dwivedi 2021).
137 Some of these miRNAs are localized at the synapse and have been shown to regulate
138 synaptic plasticity and memory (Mckibben and Dwivedi 2021). A recent study from our
139 laboratory has identified a set of synapse-enriched lncRNAs from the hippocampus.
140 Among these transcripts, a specific lncRNA has been shown to regulate hippocampus-
141 dependent memory (Samaddar et al., 2023). LncRNA functions as scaffolds, decoys,
142 guides, or enhancers to modulate chromatin remodelling, transcription, mRNA
143 stability, and RNA-protein interactions (Mattick et al., 2023; Mercer et al., 2009).
144 Recent attention has focused on lncRNA activity at synapses that govern synaptic
145 plasticity, neuronal development, and neurological disorders (Zhang, Hamblin, and Yin
146 2017) (Shi, Zhang, and Qin 2017) (A. Wang et al. 2017). The regulatory function of
147 lncRNA has also been attributed to anxiety (Spadaro et al. 2015) and memory
148 (Soutschek et al. and Schratt et al., 2023; Cui et al., 2022).

149 Prompted by these observations, we have investigated the impact of MS on the
150 expression of lncRNAs and their involvement in MS-induced anxiety and memory. Our
151 study identifies that MS enhances the expression of the lncRNA Gas5. The knockdown
152 of Gas5 alone shows no significant changes in spine development in adult mice.
153 However, when accompanied by early-life stress, Gas5 RNAi partially alleviates the
154 enduring consequences of the stress as detected by the reduction in anxiety and the
155 occlusion of memory deficits following MS.

156

157

158

159

MATERIAL AND METHODS

Animal ethics, acquisition, and maintenance

All animals were issued from the National Brain Research Centre (NBRC) animal house facility from the protocol numbers NBRC/IAEC/2015/171, NBRC/IAEC/2015/172 and NBRC/IAEC/2015/178 approved by IAEC (Institutional Animal Ethics Committee) of NBRC registered with the CPCSEA (Committee for the Purpose of Control and Supervision of Experiments on Animals) (Registration number: 464/GO/ReBi-S/Re-L/01/CPCSEA), Government of India.

Animals were housed in standard housing facilities in cages with food water *ad libitum*. A temperature of around 24± 0.5 °C and humidity of 40 ± 5% was maintained along with a 12-hour light/dark cycle for all animals.

Maternal Separation

In our study, we have focused on the aspects of induction of stress only due to maternal separation and not early social isolation, where pups are separated from the mother as well as from each other (Alves et al., 2022). The maternal separation paradigm was used as a chronic early-life stress paradigm for C57BL/6 mice pups (Sood et al. 2018). A litter size of 5-7 pups was selected for the experiment. 1 litter of pups or 1 dam was considered 'N' and was arbitrarily allocated into homecaged (HC) and maternally separated (MS) groups. A total of 32 dams (120 pups (n)) were used for maternal separation throughout the study. Postnatal day 2 (P2) pups were separated from their mother for a period of 3 hours (0900 to 1200) till P14. The mother was first moved into a different fresh cage and kept in a separate room. The pups were then placed in a beaker with soft bedding and protective paper lining and the temperature was maintained at 37˚C throughout separation. After 3 hours, first, the pups were kept back in the original cage followed by the mother. No separation was done from P15 till weaning on P21. Handling of the pups was done very gently. Cage changes were done every three days starting from P4. For the control group, designated as HC, all litters and mothers were kept undisturbed from P0 to P21 except for regular maintenance and cage changes every three days. Male pups were

190 sacrificed at P21 (euthanization with CO_2 gas), and hippocampi were isolated for
191 further biochemical processes.

192 **Screening of Lnc RNAs**

193 P21 male and female pups (N=14) were sacrificed in a CO_2 euthanasia chamber at a
194 30-70% fill rate of CO_2 gas and death was confirmed by tail/feet pinch and lack of
195 respiration. Euthanasia was followed by a quick decapitation of the animals and the
196 whole hippocampi was harvested in Trizol reagent (Invitrogen) for total RNA isolation.
197 SuperScript III First Strand Synthesis System (Life Technologies, Invitrogen) kit was
198 used for synthesizing cDNA following the manufacturer's protocol. Further, qPCR of
199 the cDNA prepared was done using SyberGreen (Applied Biosystems). See Table 1
200 for qPCR primer details.

201 TABLE 1. Primers for qPCR

No	LncRNA	Forward Primer (5' – 3')	Reverse Primer (5' – 3')
1	Tubulinβ-1	GCGCCTTTGGACACCTATTCA	CCGCGCCCTCCGTATAGTGC
2	GAPDH	CGTATTGGGCGCCTGGTCAC	CGGCCTCACCCCATTTGATG
4	Gas5	AGGAGGATGAAGGCTTACGA	AACTGTCTATCCAGCCTCAA
5	Pvt1	TTGCCTGGAGATGTTACAAG	AACATTCTCATTGAGTCAAG
6	SynLAMP (2410006H16Rik)	AAGAGTGGAAGATTGCCAAC	GATTACCAAATGTGCCCACC
7	2900052NO1 Rik	ACAATCCAAATCTACCCACGAG	TGGGATTGTAGATTGTGCTGTC
	1700020IRik	TGACTGCATCTCCGAGGAAT	GGCCTGCTACTATTGCTTACA
9	Zfas1	CGCCGCCAAGGTCTATATAA	CAGGTCAACCATCTGCAAGT
10	Pantr1	ATTTCCTGAGTCAACATGGC	AGAGTATGCCACATGGATGAT G
11	Snhg8	CAGTGGAGGAAGTGTTAAGGT	CCACTACAGTACCTGCAAGAA
12	Snhg12	TCTCCGGATGATTCGTGAGA	TCTGCTGTATCGTTGTCCAT
13	Rmst1	CATGAATGTTGTCGACACTGT	GAGCTTGGCAGATCCTTCAA

202

203 **Cloning and Virus preparation**

204 EF1-α promoter from pLVTHM (Addgene # 12247) was used to replace the CMV
205 promoter in pAAV.U6.shRLuc.CMV.ZsGreen.SV40 (Penn Core Vector) plasmid by
206 excising out the CMV promoter using the EcoRI (NEB #R3101) and NHE-I (NEB
207 #R3131) cut sites. Infusion cloning (Takara-Bio In-Fusion HD cloning Kit; 639650) was
208 used to clone in EF1-alpha promoter generating a pAAV.U6.shRLuc.EF1-
209 α.ZsGreen.SV40 plasmid and express ZsGreen under EF1-α promoter (Table 2).
210 Universal Control (UC) and Gas5 shRNAs (shRNA # 1= G5C1 and shRNA # 2= G5C2)
211 were cloned by replacing the existing Luciferase shRNA (shRLuc) under a U6
212 promoter using BamHI (NEB #R0136L) and EcoRI restriction sites (Table 3). The final
213 vector was coined as pAAV.U6.shRNA(UC).EF1-α.ZsGreen.SV40,
214 pAAV.U6.shRNA(G5C1).EF1-α.ZsGreen.SV40 and pAAV.U6. shRNA(G5C2).EF1-
215 α.ZsGreen.SV40 respectively.

216 ZsGreen was replaced with EGFP in all vectors to achieve a diffused fluorescence for
217 imaging. All vectors were digested with NcoI-HF (NEB #R3193) and NotI-HF (NEB
218 #R3189) to excise out ZsGreen. EGFP from the pLVTHM vector was inserted by
219 infusion cloning (Table 4).

220 All clones were verified by Sanger sequencing.

221 TABLE 2. Infusion primers for replacing CMV with EF1-α in AAV backbone

No.	Primers 5'-3'	Oligo sequence
1.	Forward	TTTTACGCGTGAATTCGGCTCCGGTGCCCGTCAG
2.	Reverse	GACCGGTAGCGCTAGCTCACGACACCTGAAATGGAAG

222

223

224 TABLE 3. shRNA Antisense Sequence

No.	Lnc-RNA	Oligo Sequence (5' – 3')
1.	UC shRNA	ATCTCGCTTGGGCGAGAGTAAG
2.	G5C1 shRNA	GAGGCTGGATAGACAGTTTGA
3.	G5C2 shRNA	GGTCCTTCATTCTGAATTTCA

225

226

227 TABLE 4. Infusion primers for replacing ZsGreen with EGFP in AAV backbone

No.	Primers 5'-3'	Oligo sequence
1.	Forward primer 5'-3'	CCGGTCGCCACCATGATGGTGAGCAAGGGCGAGG
2.	Reverse primer 5'-3'	CTGCTCGAAGCGGCCCTTGTACAGCTCGTCCATGCC

228

229 The expression vector was propagated using the *E.coli* Stbl3 strain and the AAV
230 packaging plasmids pAdDeltaF6 and pAAV2.9 (Penn vector Core) were propagated
231 using the DH5α strain. Endotoxin-free Maxiprep kit (Qiagen) was used to prepare
232 purified plasmid for HEK293T cell transfection. Calcium phosphate transfection was
233 done using 10μg of the above-mentioned transfer vector, 10μg pAAV2/9n and 20μg of
234 pAdDeltaF6 into HEK293T cells of density $2X10^6$ cells. The culture was maintained at
235 37℃, 5% CO_2 in low-glucose DMEM (Gibco) with 10% foetal bovine serum with one-
236 time media change after 8 hours. Post 96 hours of infection, NaCl (final concentration:
237 500 mM) was added to the plates for 3 hours to lyse the cells. The supernatant was
238 collected and stored at 4℃. The remaining cells on the plates were scraped and
239 collected separately. The cells went through three freeze-thaw cycles where they were
240 frozen at -80℃ and thawed at 37℃ for complete dissociation of virus particles from
241 the cell membrane. The filtrate was added to the supernatant collected before;
242 together they were filtered through a 100μ and a 0.45μ filter successively. The final
243 filtrate, containing the virus, was then centrifuged using Amicron-Ultra-15 (Merk
244 Millipore #UFC910024) filters to concentrate the virus and determine the titre by
245 fluorescence-based cell counter. The multiplicity of infection (MOI) was calculated by
246 infecting 80K HEK293T cells with serially diluted AAV solutions. An MOI of 1-2 was
247 used for further experiments.

248 **Primary Neuronal Culture**

249 Hippocampal neurons were cultured following the previous protocol (Kaech & Banker,
250 2006). CD1 dams were euthanized in a CO_2 gas chamber (fill rate 30-70%) followed
251 by cervical dislocation and death was confirmed by tail/feet pinch. The uterus
252 containing the embryonic day 16 (E16) pups was dissected and taken out on ice-cold
253 dissection media (Gibco) to render the pups unresponsive to painful stimuli. An incision

254 was made in the uterus to extract the pups for decapitation and the whole brain was
255 collected from the sacrificed pups. Hippocampi from all pups from a single CD1 (N=4)
256 were pooled for further experiments. Briefly, hippocampi from embryonic pups were
257 dissected and collected in dissection media (Gibco). It was then digested with the
258 addition of 2.5% trypsin to the dissection media at 37℃ for 10 mins. Trypsin-treated
259 tissue was washed with dissection media and collected in Glial Minimum Essential
260 Media (GMEM; Gibco). Further, trituration was done with a fire-polished Pasteur
261 pipette to obtain a single-cell suspension which was plated on poly-L-lysine coated
262 60mm dishes (1 mg/mL, Sigma) at a concentration of 200-250 cells/mm^2. The culture
263 was maintained at 37℃, 5% CO_2 in Neurobasal Media (Gibco) with B27 supplement
264 (Gibco) throughout the experiment. Cells were infected with AAV at DIV 7 and
265 harvested at DIV 21 for further experiments.

266

267 **Stereotaxic injection**

268 Surgery was done in P0 pups (N=56, n=168) 6-8 hours post-birth only after the
269 appearance of the milk spot (Kim et al. 2014). Half of the litter was taken at a time and
270 kept on a heating pad at 37˚C. For anaesthesia, the pup was kept on a cold metal
271 plate kept on the ice for 2-3 mins till there was no movement and the body colour
272 turned whitish pink from reddish pink. It was then lightly taped to the platform with its
273 head erect. The platform was kept at 7-8℃ to maintain the anaesthesia. In case the
274 pup's body colour started to show a bluish tinge, the temperature was raised to 12-
275 15℃. Stereotaxic arms were moved to (X, Y) = (0.8, 1.5) mm coordinates and the
276 needle was lowered till at Z= -1.8 mm (Christensen et al. 2010). Each hippocampus
277 was injected with 0.5 µl of AAV with MOI=1. A volume of 0.1 µl was injected per minute
278 with a gap of 10 mins. On completion of 0.5 µl virus injection, an additional gap of 10
279 mins was given before the needle was pulled out very slowly to prevent any back
280 suction. We proceeded to inject into the second hippocampus after 15 minutes during
281 which the first wound site was allowed to close. The pup was then kept on a 37℃
282 heating pad and warmed till movement and colour were regained. They were returned
283 to the mother together to minimise disturbances. The cage was left completely
284 undisturbed for the next day. (n=163; surgeries performed for western blot, spine

analysis, light dark assay, spatial object recognition assay. ‘n’ determines the number of individual animals; males).

Light/dark box assay

The apparatus consists of a smaller dark box with a light intensity of 2 Lux (one-third of the total area) and a bigger light box with a light intensity of 390 Lux (two-thirds of the total area) separated by a door (Bourin and Hascoët 2003) (Takao and Miyakawa 2006). P42 mice (N=26, n=79) were habituated for 2 minutes to handling and to a transport vessel in dim light (2-5 Lux) for 1 week in the experimental room. Animals were housed in standard cages and a 12-hour light/dark cycle was maintained as usual. On test day, the mouse was kept in the dark box with a closed door. The door was opened 10 seconds later and the mouse was left free to explore the light box for 10 minutes. The behaviour assays and habituations were performed between 0900 hours to 1800 hours. Arenas were cleaned using 70% alcohol between tests to prevent any odour-related bias (Takao and Miyakawa 2006). The video was recorded using a Logitech HD webcam C270 overhead-mounted camera and analysed using online free software (Toxtrac) (Rodriguez et al. 2018), which was also blind tested manually. The total distance covered, time spent in the light box, and the number of transitions made between the two boxes were considered. The litter effect for animals used in light/dark box assay was also analysed (Figure S 3A-C).

Spatial object recognition assay

All animals were housed in single cages a week before the experiment. P50 male (N=27, n=84) C57Bl/6 mice were habituated for 2 minutes to handling and a transport vessel for 1 week followed by spatial object recognition assay which comprised a total of 5 sessions, each 10 minutes long. The process is similar to the classical object recognition assay with a few variations (Wimmer et al. 2012). A light intensity of around 15 Lux was maintained at the centre of the arena (Leger et al. 2013). Session 1 involved introducing the animal to the empty arena (12 cm X 15 cm with spatial cues) for short habituation to the open field. In sessions 2 to 4, the animal was trained to explore two objects of different shapes kept in their fixed coordinates, with a 5 cm gap

316 between wall and object, through all the sessions. The animal was returned to its
317 original cage for 5 minutes to relieve stress and the arena and objects were wiped with
318 70% alcohol between each session. The test session (5th session) was carried out
319 after 24 hours of the training sessions when only one object was moved to a new
320 coordinate with leu to the spatial cues and the animal was allowed to inspect for 10
321 minutes. All recordings were done using a Logitech HD webcam C270 overhead-
322 mounted camera and a MATLAB-based autotyping software was used to calculate the
323 number of bouts on each object (T. P. Patel et al. 2014), which was also blind tested
324 manually. A bout was considered when the animal moved its nose within a space 2 cm
325 radially from the object. Any attempt to climb or jump on the object was not considered
326 a bout. The Discrimination Index (DI), which is the ratio of the difference in time spent
327 with either object to the total time spent with both objects during the test session, was
328 calculated to verify the ability of the animal to successfully recognize the displaced
329 object (Denninger, Smith, and Kirby 2018).

330 DI= [time spent with object displaced- time spent with not displaced]/ [time spent with
331 displaced+ time spent with not displaced]

332 The litter effect for animals used in spatial object recognition assay was also analysed
333 (Figure S 3D).

334

335 **Cryo-sectioning**

336 Following behaviour assessments, animals underwent sacrifice at P60 (N=53, n=163).
337 Mice were sedated with a heavy dose of Ketamine (60mg/kg) and Xylazine (10mg/kg)
338 cocktail injected intraperitoneally. They were perfused intracardially with a solution of
339 1XPBS (phosphate buffer saline) followed by 4% paraformaldehyde, for maintaining
340 tissue integrity. To ensure thorough fixation, brains were extracted and immersed in
341 4% paraformaldehyde for an additional 5 days post-perfusion. Subsequently, the fixed
342 brains were incubated in 40% sucrose solution for a week till they settled to the bottom,
343 enabling optimal cryo-sectioning. Brains were flash-frozen in dry ice and coronal
344 sections of 50µ thickness were obtained and mounted on slides pre-coated with
345 gelatin. The tissue sections were washed 3 times with autoclaved Mili-Q water and
346 mounted with Vectasheild DAPI to stain the nucleus and visualized under the
347 microscope.

348

349

350 **Spine analysis**

351 To measure neuronal development, recombinant AAV expressing two distinct shRNAs
352 were injected into the hippocampus of male mice (P0) (N=3, n=5) and these neurons
353 were imaged at P38-P40 (16-bit) using a Nikon A1 HD25 point scanning confocal
354 microscope with Nikon Plan Apochromat NA=1.4 oil immersion objective at
355 1024X1024 pixel resolution at 0.75X. 2X optical zoom was used to get high-
356 magnification images of neurons with 10 -15 optical sections with 0.25µm step size.
357 The GFP signal was captured by a 488 nm solid-state laser. Images were obtained
358 under uniform parameters of laser power; pinhole diameter and detector gain across
359 all conditions (Figure 6A-B).

360 Neurolucida 360 (MBF Bioscience) was used for spine morphology analysis. A 3-D
361 skeletal image was generated using the Directional Kernel tracing algorithm and
362 spines were detected and classified. Spine density was obtained by using Neurolucida
363 Explorer (Figure 6C-E).

364 Coronal sections of the mouse brain were visualized using a Leica LAS V4.2
365 fluorescence microscope and Zeiss Apotome3 (magnified image) (Figure S 1G-H). All
366 imaging parameters were kept uniform across experiments. Images were stitched
367 post-acquisition using Fiji image analysis software (MosaicJ plugin).

368

369 **Western blot**

370 The hippocampal tissue was obtained from C57BL/6 male P21 pups (N=8, n=25),
371 previously subjected to injections of UC, G5C1, or G5C2 shRNAs at P0. The pups
372 were euthanized in a CO_2 chamber at a 30-70% fill rate of CO_2 gas and death was
373 confirmed by tail/feet pinch. The tissue was lysed in RIPA buffer (composed of 150mM
374 NaCl, 0.1% NP-40, 0.5% sodium deoxycholate, 0.1% SDS, 50 mM Tris, pH 7.4) and
375 subsequently centrifuged at 4°C for 10 minutes at 4000 g to remove debris. Protein
376 quantification was performed using the Pierce BCA Protein Assay Kit (Thermofisher)
377 with the resulting clear supernatant.

For experimental purposes, specific sample lysates were mixed with Laemmli Buffer and heated to 95°C. An amount of 5 µg of each sample was utilized for housekeeping gene tubulin-β1 (Tuj-1) blot, while 30 µg of each sample was employed for pan-Ago blot. The samples were resolved by electrophoresis on a 10% polyacrylamide gel and then transferred onto a nitrocellulose membrane. Subsequently, the membrane was blocked with 5% BSA and incubated with primary antibodies against Tuj-1 (dilution 1:10,000, Sigma, Catalog # T8578) and pan-Ago (dilution 1:1200, MerkMillipore, Catalog # MABE56) overnight at 4°C. Following the primary antibody incubation, the membrane was washed 6 times, 10 minutes/wash, with 1X TBST (Tris-buffered saline with 1% Tween 20) at RT. The blot was then exposed to secondary antibodies (dilution 1:10,000 for Tuj-1 and 1:5000 for pan-Ago, Goat Anti-Mouse, Thermofisher Scientific, Catalog# A11030) for 3 hours. Further washing was done with 1X TBST (6 washes, 10 minutes/wash) to obtain cleaner background. Luminescence on the blot was detected using the ECL chemiluminescence kit (Millipore). Band intensities and the expression of pan-Ago were quantified using ImageJ software, with normalization against tubulin-β1.

Statistics

Statistical analyses were performed for all experiments. Data shown are represented as mean±SEM. The number of pregnant dams/ litters used is defined by ‘N’ and the total number of pups (obtained from the dams) used is designated as ‘n’. The number of neurons considered for spine analysis is represented as ‘*n”*. qRT-PCR data for lncRNA screening, Argonaute (Ago) immunoblots and spine density were analyzed using unpaired Student’s t-test with Welch’s correction for unequal variance. qRT-PCR data for Gas5 knockdown efficiency were analyzed using paired Student’s t-test. Two-way ANOVA with Fisher’s LSD test was used for analyzing light/dark and SOR data analysis. GPower 3.1 was used for post-hoc power analysis for all experiments. The outlier test was done using the ROUT method (0.1% aggressive). Immunoblot band intensity analysis and image stitching were done using ImageJ software. Gene Ontology plots were computed using RStudio (Figure 5 A-C) and SRplot (Figure 7 B-E) (Tang et al. 2023). Data with a p-value less than 0.05% were considered significant. All data were analysed using GraphPad Prism 9. No randomisation technique was

410 used animals were grouped arbitrarily. No prior sample size was calculated. Post-hoc
411 power analysis was done for all experiments. Detailed statistical analysis and criteria
412 for the exclusion of animals is provided in Supplementary data and Figure S5.

413

414 **RESULTS**

415 **Maternal separation alters the differential expression of synapse-enriched**
416 **lncRNAs**

417 To investigate the impact of early life stress, this study used the maternal separation
418 (MS) paradigm (Figure 1A) and the differential expression of a subset of synapse-
419 enriched lncRNAs was analyzed by qPCR in males and females separately. In males,
420 we observed a significant upregulation in the expression of specific lncRNAs, such as
421 Pantr1 (146.3 ± 56.78% increase, p=0.041) and Gas5 (79.6 ± 19.14% increase,
422 p=0.006) and without any change in expression of 1700020I14Rik (8.30 ± 13.14%
423 increase, p=0.5522) upon MS. Although, we observed an increase in expression of
424 2410006H16Rik (105.5 ± 75.28% increase, p=0.210), 2900052NO1Rik (100.3 ±
425 70.88% increase, p=0.206), Pvt1 (82.9 ± 46.95% increase, p=0.127), RMST_1 (49.9
426 ± 51.05% increase, p=0.366), Snhg6 (95.4 ± 81.12% increase, p=0.284), Snhg8 (80.5
427 ± 73.63% increase, p=0.316), Snhg12 (86.3 ± 48.60% increase, p=0.126) and Zfas1
428 (37.4 ± 23.57% increase, p=0.163); these enhancement in expression are not
429 statistically significant (Figure 1B). Gas5 was selected as the target lncRNA and two
430 shRNAs (G5C1 and G5C2) against Gas5 were cloned into an AAV vector (Figure
431 S1A). Knockdown efficacy was assessed in primary hippocampal neuronal culture and
432 successful knockdown was evaluated for both the constructs (82.82 ± 9.33 %
433 decrease, p= 0.003 for G5C1 and 84.93 ± 13.68 % decrease, p= 0.25 for G5C2 w.r.t
434 GAPDH; 81.3 ± 8.46 % decrease, p=0.0024 for G5C1 and 83.71 ± 6.9 % decrease,
435 p=0.0067 for G5C2 w.r.t Tubulin-β1) (Figure S1C-D).

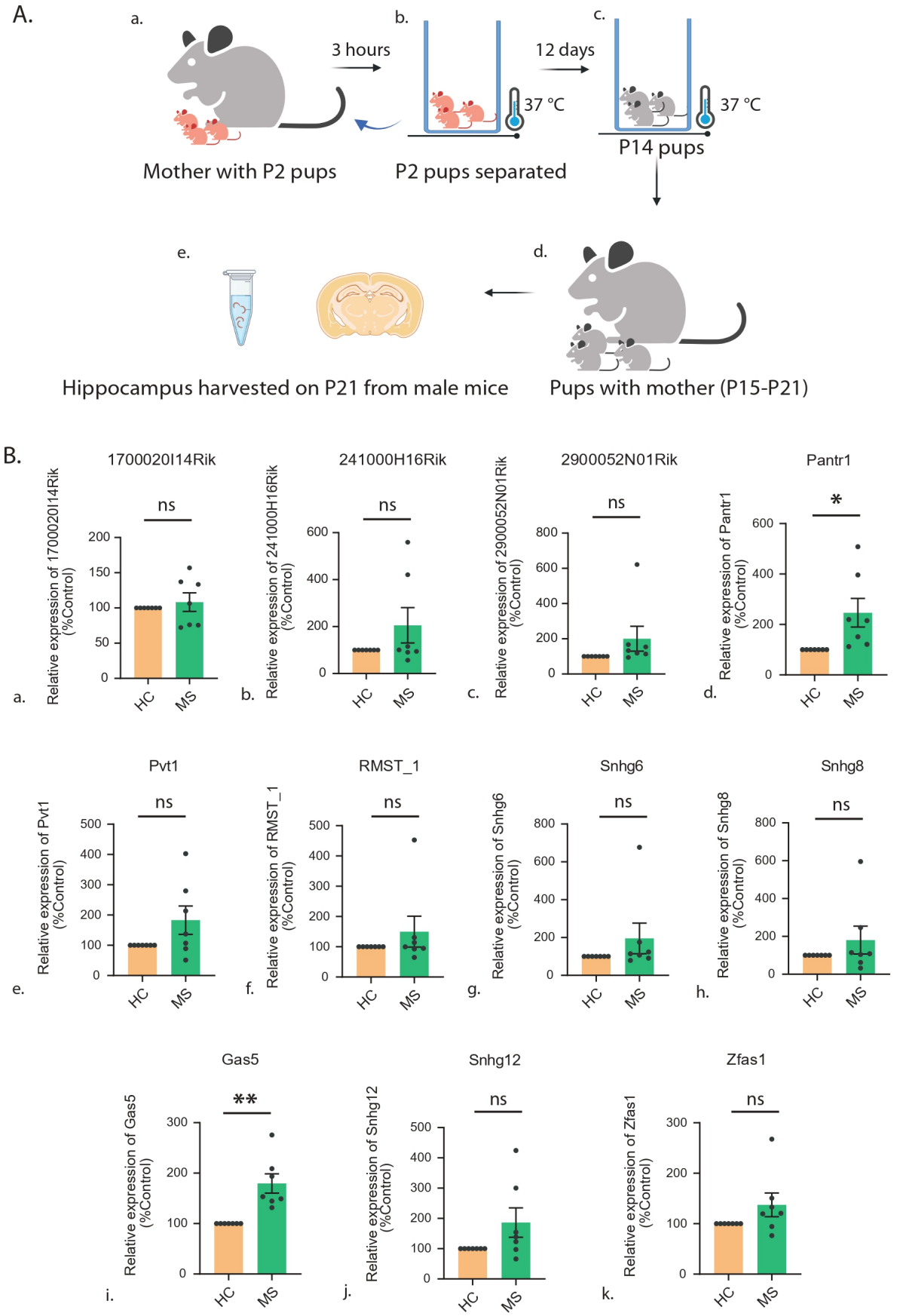
A.
a.
3 hours
b.
12 days
c.
37 °C
37 °C
Mother with P2 pups
P2 pups separated
P14 pups
e.
d.
Hippocampus harvested on P21 from male mice
Pups with mother (P15-P21)
B.
1700020I14Rik
241000H16Rik
2900052N01Rik
Pantr1
Pvt1
RMST_1
Snhg6
Snhg8
Gas5
Snhg12
Zfas1
Relative expression of 1700020I14Rik (%Control)
Relative expression of 241000H16Rik (%Control)
Relative expression of 2900052N01Rik (%Control)
Relative expression of Pantr1 (%Control)
Relative expression of Pvt1 (%Control)
Relative expression of RMST_1 (%Control)
Relative expression of Snhg6 (%Control)
Relative expression of Snhg8 (%Control)
Relative expression of Gas5 (%Control)
Relative expression of Snhg12 (%Control)
Relative expression of Zfas1 (%Control)
ns
*
**
HC
MS

436

Figure 1. Maternal separation affects the expression of synapse-enriched lncRNAs. (**A**). Maternal separation paradigm followed: P2 pups separated from their mother for 3 hours during P2 – P14 and following MS pups were kept till P21. (**B).** Differential expression of synapse-enriched lnc-RNAs in male hippocampus (P21) (a) 1700020I14Rik, (b) 2410006H16Rik, (c) 2900052NO1Rik, (d) Pantr1, (e) Pvt1, (f) RMST_1, (g) Snhg6, (h) Snhg8, (i) Gas5, (j) Snhg12, (k) Zfas1 as obtained through qPCR, *p < 0.05, **p < 0.01, ns = not significant. N=7, Data shown as mean ± SEM. Unpaired Student's t-test with Welch's correction.

The underlying data is also shared in https://figshare.com/articles/dataset/_b_Gas5_regulates_early_life_stress-induced_anxiety_and_spatial_memory_b_/26047969 .

In females, no significant alteration of Gas5 expression was seen after MS (24.77 ± 21.91, p= 0.3095). A significant downregulation of Zfas1 (47.50 ± 5.535, p= 0.0004) was observed. 2900052NO1Rik (164.9 ± 54.88, p= 0.0300), Snhg6 (101.9 ± 39.48, p= 0.0494) and Snhg8 (19.09 ± 6.565, p= 0.0335) were significantly upregulated upon MS. Other lncRNAs like 1700020I14Rik (5.670 ± 10.08, p= 0.5982), 2410006H16Rik (-28.74 ± 16.25, p= 0.1373), Pantr1 (-13.13 ± 18.85, p= 0.5172), Pvt1 (-20.40 ± 18.66, p= 0.3241), RMST_1 (219.2 ± 210.8, p= 0.3460) and Snhg12 (-5.823 ± 37.76, p= 0.8835) were not differentially regulated in the hippocampus after early life stress. The data showed the sexual dimorphic expression of lncRNAs between males and females.

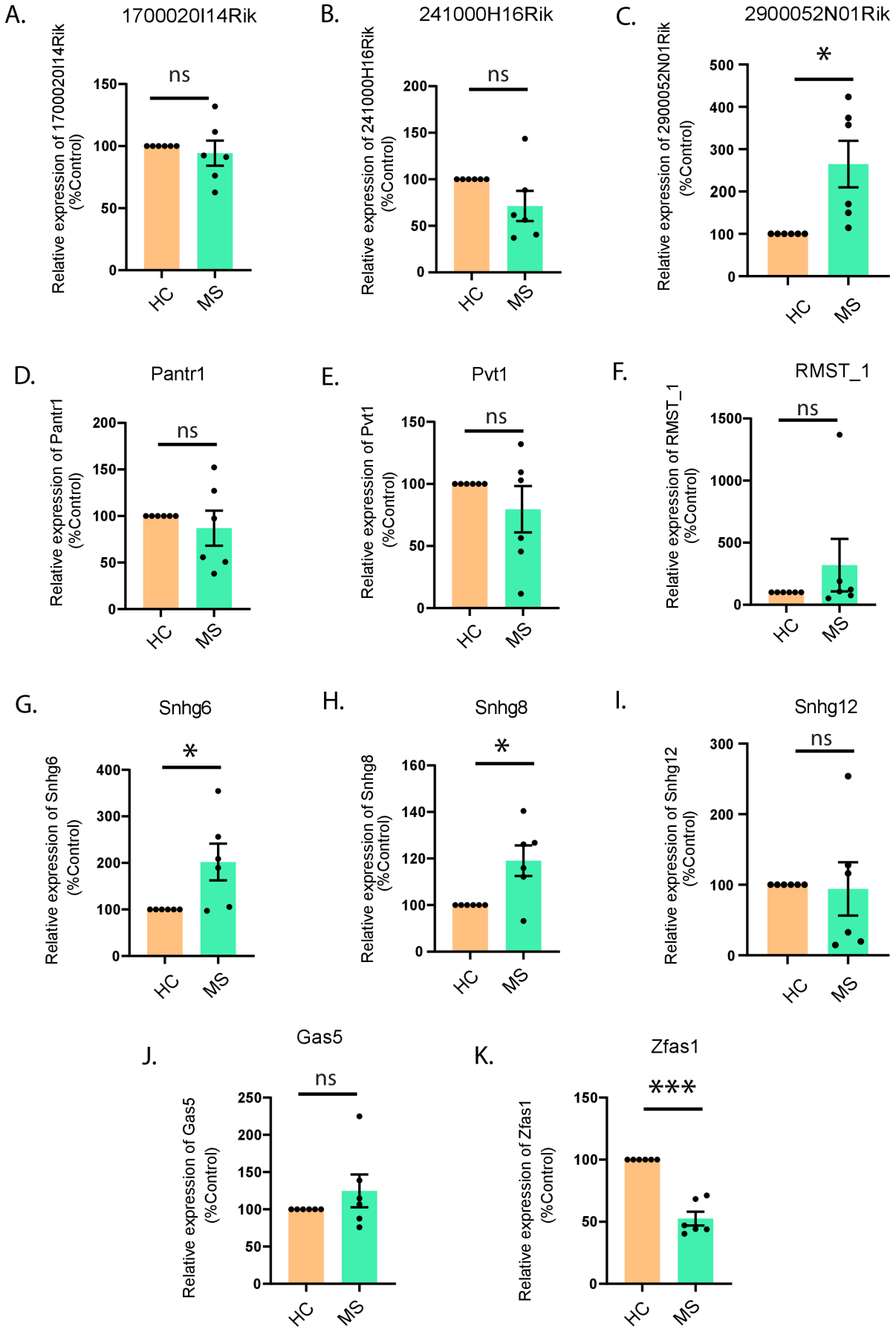
A.
1700020I14Rik
Relative expression of 1700020I14Rik (%Control)
ns
150
100
50
0
HC
MS
B.
241000H16Rik
Relative expression of 241000H16Rik (%Control)
ns
200
150
100
50
0
HC
MS
C.
2900052N01Rik
Relative expression of 2900052N01Rik (%Control)
*
500
400
300
200
100
0
HC
MS
D.
Pantr1
Relative expression of Pantr1 (%Control)
ns
200
150
100
50
0
HC
MS
E.
Pvt1
Relative expression of Pvt1 (%Control)
ns
150
100
50
0
HC
MS
F.
RMST_1
Relative expression of RMST_1 (%Control)
ns
1500
1000
500
0
HC
MS
G.
Snhg6
Relative expression of Snhg6 (%Control)
*
400
300
200
100
0
HC
MS
H.
Snhg8
Relative expression of Snhg8 (%Control)
*
160
140
120
100
0
HC
MS
I.
Snhg12
Relative expression of Snhg12 (%Control)
ns
300
200
100
0
HC
MS
J.
Gas5
Relative expression of Gas5 (%Control)
ns
250
200
150
100
50
0
HC
MS
K.
Zfas1
Relative expression of Zfas1 (%Control)
***
150
100
50
0
HC
MS

461

462 **Figure 2. Maternal separation affects the expression of synapse-enriched lncRNAs in**
463 **hippocampus of female P21 mice**. Differential expression of synapse-enriched lnc-RNAs
464 (A). 1700020I14Rik (B)2410006H16Rik, (C) 2900052NO1Rik, (D) Pantr1, (E) Pvt1, (F)
465 RMST_1, (G) Snhg6, (H) Snhg8, (I) Snhg12, (J) Gas5, (K) Zfas1 as obtained through qPCR,
466 *p < 0.05, **p < 0.01, ns = not significant. N=6, Data shown as Mean ± SEM. Unpaired
467 Student's t-test with Welch's correction.

468 The underlying data is also shared in
469 https://figshare.com/articles/dataset/_b_Gas5_regulates_early_life_stress-
470 induced_anxiety_and_spatial_memory_b_/26047969 .

471

472

473 **Gas5 knockdown partially alleviates MS-induced anxiety**

474 We have analysed open-space anxiety of mice that are injected with AAV expressing
475 shRNAs against Gas5 or non-targeting control. Mice were bilaterally injected with AAV
476 expressing either G5C1 or G5C2 in the hippocampus at P0. These mouse pups were
477 maternally separated or homecaged (P2 – P14); following which they were kept with
478 their respective mother till P21 (day of weaning). Young-adult male mice (P48) were
479 subjected to the light/dark box assay (Figure 3A) (X. Wang et al. 2022). Maternally
480 separated mice exhibited avoidance of brightly-lit open areas as detected by
481 subsequent reduction in time spent (102.2 ± 24.35 second (s) decrease, p<0.0001);
482 distance covered (18.26 ± 2.814 meters (m) decrease, p<0.0001), and fewer
483 transitions (13.55 ± 3.55 decrease, p= 0.0003) into the brightly lit arena as compared
484 to the homecaged control. However, the maternally separated Gas5 RNAi mice
485 showed a partial rescue in anxiety level as measured by time spent (65.47 ± 27.03 s
486 increase, p= 0.0179 for G5C1 and 66.62 ± 25.21 s increase, p<0.0101 for G5C2),
487 distance covered (17.45 ± 3.123 m increase, p <0.0001 for G5C1 and 13.38 ± 2.912
488 m increase, p<0.0001 for G5C2) and number of transitions (11.42 ± 3.943 increase,
489 p= 0.005 for G5C1 and 8.615 ± 3.677 increase, p=0.0219 for G5C2) into the brightly
490 lit arena with respect to maternally separated mouse expressing non-targeting control
491 shRNA (Figure 3C-E). We have also observed that homecaged mice expressing Gas5
492 shRNA did not show any change in time spent, distance covered and the number of
493 transitions into the brightly lit arena as compared to homecaged mice expressing non-
494 targeting shRNA (Figure 3C-E). These observations indicate that Gas5 RNAi does not

495 alter any physiological phenotype of the animal. Litter effect was also statistically
496 analysed and no significant difference in behaviour among the litters was found (Figure
497 S 3 A-C).

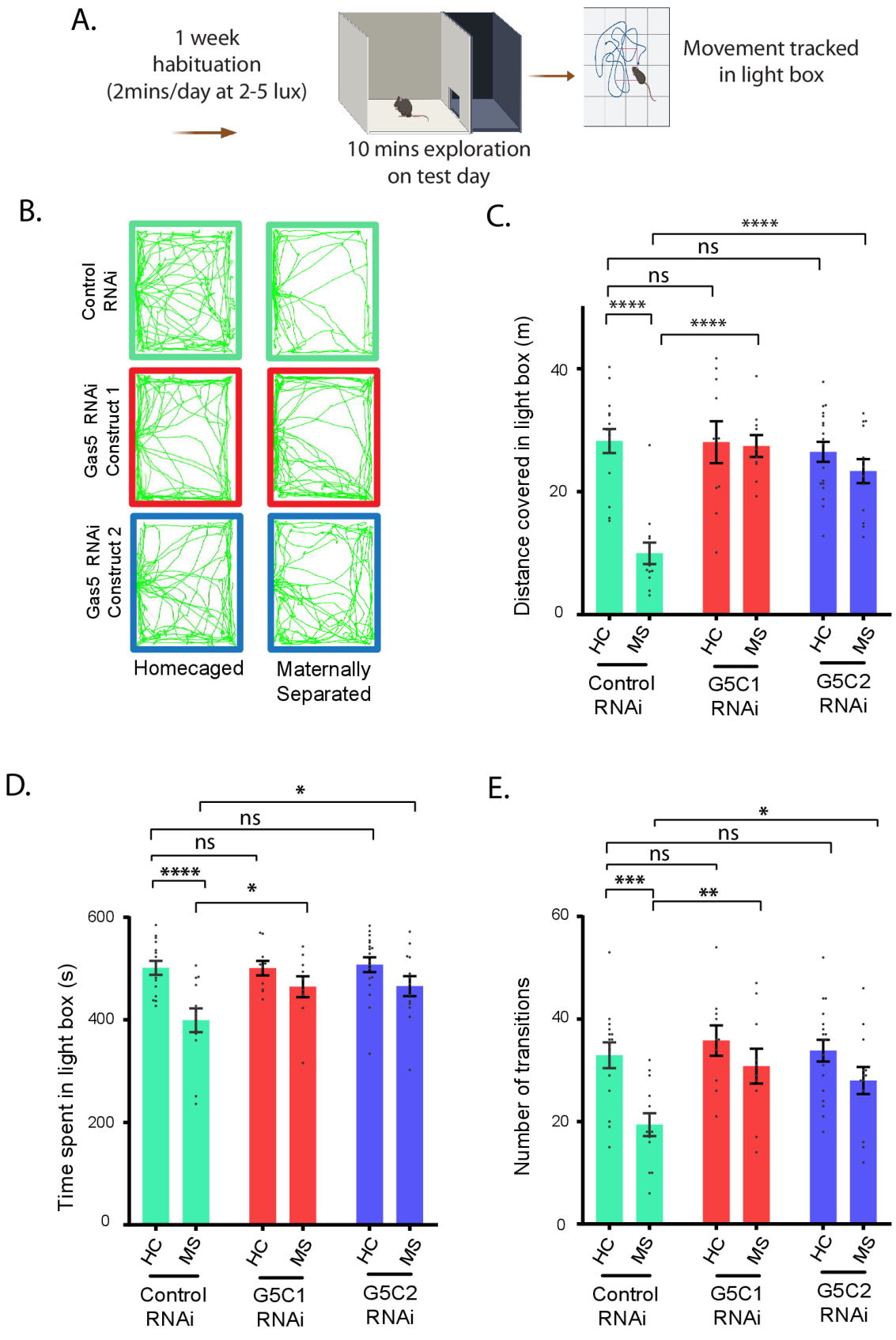
A.
1 week
habituation
(2mins/day at 2-5 lux)
10 mins exploration
on test day
Movement tracked
in light box
B.
Control
RNAi
Gas5 RNAi
Construct 1
Gas5 RNAi
Construct 2
Homecaged
Maternally
Separated
C.
Distance covered in light box (m)
0
20
40
****
ns
ns
****
****
HC
MS
HC
MS
HC
MS
Control
RNAi
G5C1
RNAi
G5C2
RNAi
D.
Time spent in light box (s)
0
200
400
600
*
ns
ns
****
*
HC
MS
HC
MS
HC
MS
Control
RNAi
G5C1
RNAi
G5C2
RNAi
E.
Number of transitions
0
20
40
60
*
ns
ns
***
**
HC
MS
HC
MS
HC
MS
Control
RNAi
G5C1
RNAi
G5C2
RNAi

498

499

500 **Figure 3. Gas5 knockdown reduces anxiety following maternal separation. A**. Paradigm
501 depicting light/dark box assay to measure anxiety. **B**. Representative trace showing the
502 movement of the mouse in the bright-lit arena in the light/dark box. **C.** HC = Homecaged, MS
503 = Maternally Separated, G5C1= shRNA # 1, G5C2 = shRNA # 2. Distance covered in the light
504 box (in meters). **D.** Time spent in the light box (in seconds). **E.** Total number of transitions
505 made between light and dark box. Data shown as mean±SEM, N=3-7, n=10 - 18, *p<0.05 **p<
506 0.01, ***p<0.005, ****p<0.0001, ns not significant. Two-way ANOVA with Fisher's LSD test.
507 The underlying data is also shared in
508 https://figshare.com/articles/dataset/_b_Gas5_regulates_early_life_stress-
509 induced_anxiety_and_spatial_memory_b_/26047969 .

510 ---

511

512 **Gas5 RNAi rescues MS-induced spatial memory deficit**

513 We have analysed the impact of early-life stress on memory using spatial object
514 recognition (SOR) test and evaluated the role of Gas5 following its knockdown (Figure
515 S1A). Mice were injected (P0) with AAV expressing shRNA against Gas5 or non-
516 targeting control. These mice were maternally separated or homecaged (P2 – P14)
517 and subjected to SOR (P56). Mice were allowed to explore two distinct objects placed
518 in two specific locations within an arena during the training session (Figure 4A, S2).
519 On the test day, 24 hours after training, one of the objects was displaced within the
520 same arena and the exploration time of non-displaced and displaced objects was
521 analysed (Figure 4A-3B). We observed that the maternally separated mice expressing
522 non-targeting shRNA displayed reduced recognition of the displaced object during the
523 test session as determined by the discrimination index (DI) (0.4152 ± 0.1204 decrease,
524 p=0.0009) when compared to the homecaged control (Figure 4D). Next, we examined
525 the effects of maternal separation on memory following the knockdown of Gas5. We
526 observed that the maternally separated mice having Gas5 RNAi could partially
527 enhance DI (0.5568 ± 0.116 increase, p<0.0001 for G5C1 and 0.5186 ± 0.1181
528 increase, p<0.0001 for G5C2) as compared to the maternally separated mice injected
529 with non-targeting control shRNA. Also, we have detected comparable DI of
530 homecaged mice injected with AAV expressing either Gas5 shRNAs or non-targeting
531 control shRNA (Figure 4D). Furthermore, the exploration of objects that were not
532 displaced within a separate arena remains unaffected following Gas5 RNAi and
533 maternal separation as we did not observe any change in DI across experimental

534 conditions (Figure 4C). These observations indicate that the reduction of Gas5
535 expression could partially rescue deficits in spatial memory following maternal
536 separation. Litter effect was also statistically analysed and no significant difference in
537 behaviour among the litters was found (Figure S 3D).

538

539 -

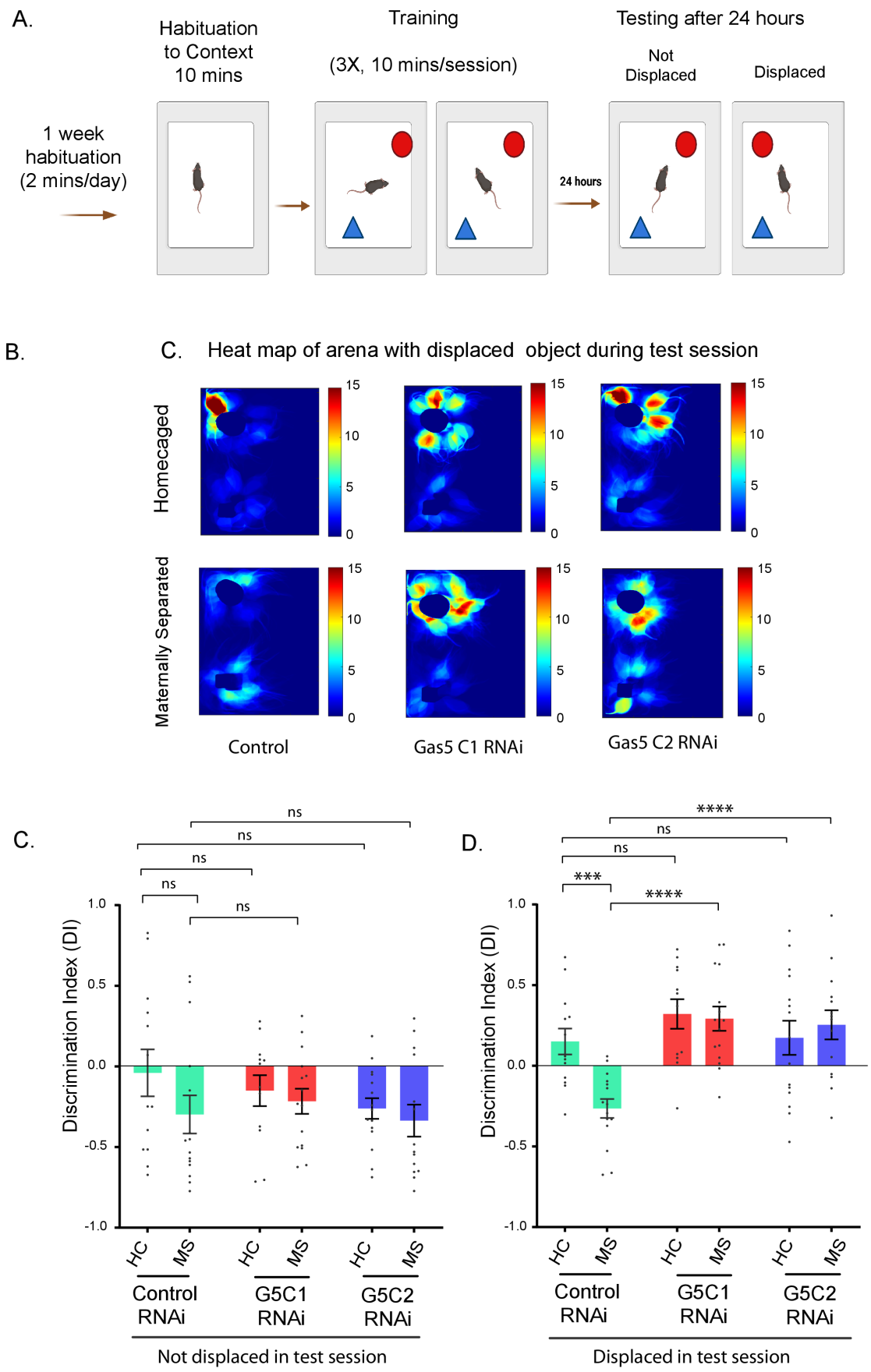
A.
Habituation to Context 10 mins
Training
(3X, 10 mins/session)
Testing after 24 hours
Not Displaced
Displaced
1 week habituation (2 mins/day)
24 hours
B.
C. Heat map of arena with displaced object during test session
Homecaged
Maternally Separated
Control
Gas5 C1 RNAi
Gas5 C2 RNAi
C.
D.
Discrimination Index (DI)
ns
***
****
HC
MS
Control RNAi
G5C1 RNAi
G5C2 RNAi
Not displaced in test session
Displaced in test session

540

541 **Figure 4. Gas5 reverses the effect of MS-induced deficits in memory**. **A.** Schematic
542 showing paradigm for SOR. **B.** Representative heat maps in the arena with the displaced
543 object during the test session, circular (glass) object represents the displaced object. **C.** HC=
544 Homecaged, MS= Maternally Separated, G5C1= shRNA # 1, G5C2= shRNA # 2.
545 Discrimination Index (DI) in the arena with no displaced object during the test session. **D.** DI
546 in the arena with a displaced object during the test session. Data shows mean±SEM. N=4-6,
547 n=12-15, *p< 0.05, **p< 0.01, ***p<0.005, ns = not significant. Two-way ANOVA with Fisher's
548 LSD test.

549 The underlying data is also shared in
550 https://figshare.com/articles/dataset/_b_Gas5_regulates_early_life_stress-
551 induced_anxiety_and_spatial_memory_b_/26047969 .

552 ---

553

554 **Gas5 is potentially involved in regulating RNA metabolism**

555 To gain a plausible mechanistic insight into the Gas5-mediated regulation of anxiety
556 and memory upon maternal separation, we took an *in silico* approach to identify the
557 expression of transcripts influenced by Gas5. First, we have selected Gas5 interacting
558 coding transcripts from the available CLIP-seq data (POSTAR3 database –
559 http://postar.ncrnalab.org./) (Hu et al. 2017). We then performed a Gene Ontology
560 (GO) analysis of these interacting coding transcripts and focused on significant
561 enrichment (FDR < 0.05) of transcripts in specific GO terms (Figure 5A-C). The cellular
562 processes included enrichment of GO-terms for ribonucleoprotein complex (FRD=
563 1.05E-31), cytoplasmic stress granule (FDR= 1.41E-17), polysome (FDR= 3.50E-05),
564 somatodendritic compartment (FDR= 0.010067571) and dendrite (FDR=
565 0.004478929) (Figure 5B) etc. The molecular functions are enriched with GO-terms
566 representing ribonucleoprotein complex binding (FDR= 1.22E-05), mi-RNA binding
567 (FDR= 6.05E-17) and translation regulator activity (FDR= 7.53E-05) (Figure 5C). The
568 biological process displays significant enrichment for GO-terms, such as RNA
569 processing (FDR= 1.58E-43), RNA splicing (FDR= 8.08E-45), regulation of translation
570 (FDR= 2.52E-18) etc. alongside some not significant but enriched terms like dendritic
571 transport of ribonucleoprotein complex (FDR= 0.094670904) and miRNA transport
572 (FDR= 0.063158655) (Figure 5A) (For details see Table S1 and Supplementary data).
573 Overall, the GO analysis revealed that Gas5 is primarily involved in RNA metabolism

574 including stability and regulation of translation. Prompted by this observation, we
575 focused on the transcript encoding Argonaute (Ago) family of proteins that are involved
576 in translation and RNA stability. As a proof-of-concept, we have analyzed the
577 expression of Ago following Gas5 knockdown. Mice were injected with AAV expressing
578 shRNA against Gas5 or UC (P0), and Ago expression in the hippocampus was
579 analyzed at P21. We observed a significant increase in Ago expression in G5C1 (0.88
580 ± 0.25 increase, p=0.0084) and G5C2 (0.78 ± 0.29 increase, p=0.0335) injected
581 animals as compared to Control RNAi individuals (Figure 5 D-E).

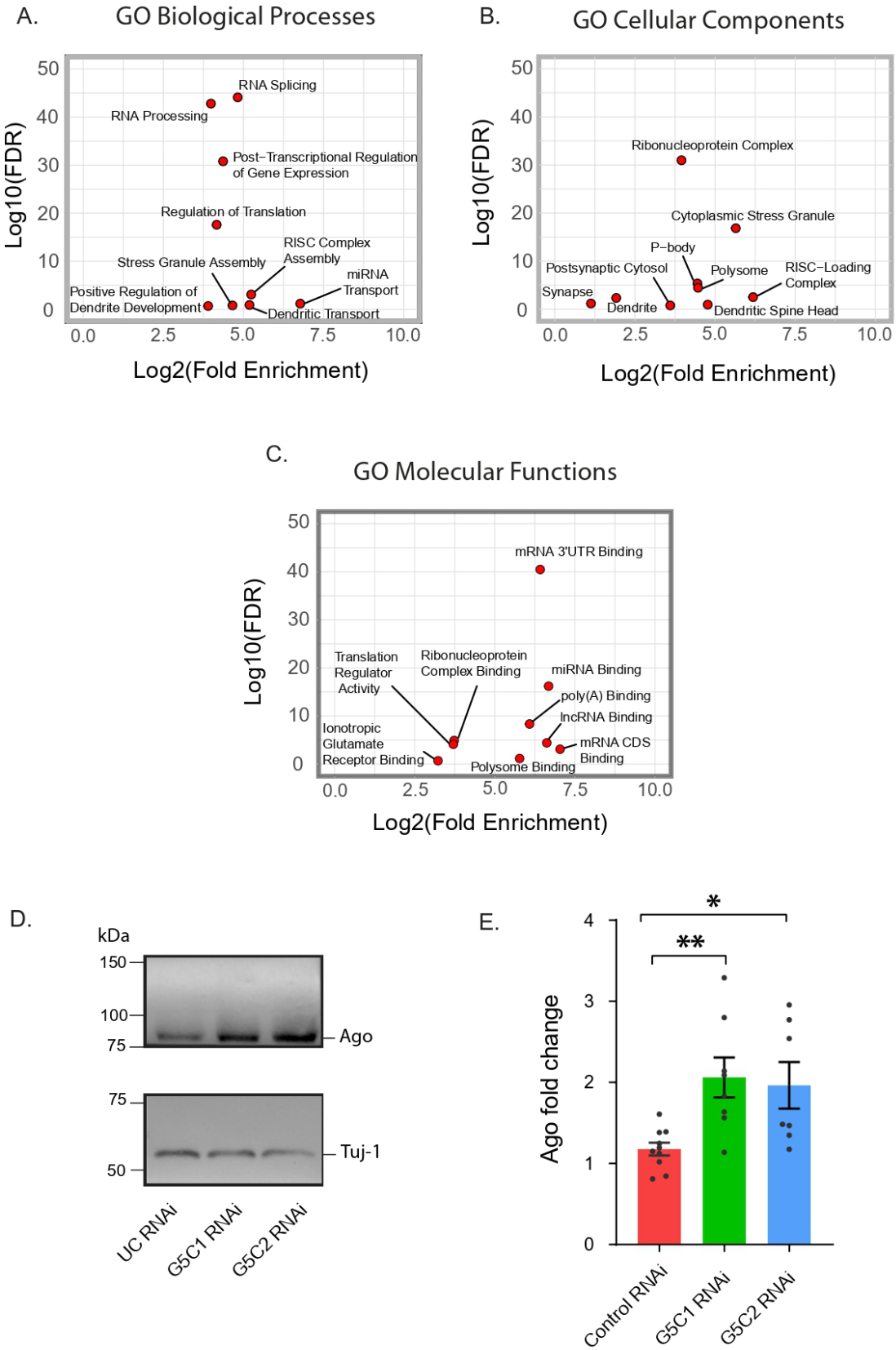

582

583 **Figure 5. Involvement of Gas5 in RNA metabolism as revealed by GO-analysis.** Available
584 CLIP-seq data of Gas5 interacting coding transcripts were used to perform gene ontology

585 (GO) analysis showing clusters of transcripts involved in **A**. Biological processes, **B**. Cellular
586 components, and **C**. Molecular functions. Red dots show significant enrichment (FDR< 0.05),
587 blue dots show highly enriched but not significant **D.** Immunoblot of Pan-Ago and Tuj-1
588 expression at the hippocampus of P21 male animals injected with Control (UC), Gas5 C1
589 (G5C1) or Gas5 C2 (G5C2) shRNA. **E.** Quantification of Pan-Ago with Tuj-1 as housekeeping
590 gene; N=2-3, n=7-10, *p<0.05; Data shows mean±SEM. Unpaired t-test with Welch's
591 correction.
592 The underlying data is also shared in
593 https://figshare.com/articles/dataset/_b_Gas5_regulates_early_life_stress-
594 induced_anxiety_and_spatial_memory_b_/26047969 .

595 ---

596

597 **Gas5 does not regulate spine development**

598 To analyse the importance of Gas5 in spine development, we effectively knocked down
599 Gas5 using two shRNAs at P0 and studied the changes in spine density at P30. We
600 studied the spine density in neurons of the CA3 region of the hippocampus. No
601 significant difference was observed in total spine density between the Control RNAi
602 and either of the Gas5 RNAi neurons (0.01281±0.05731, p= 0.825 for G5C1 and
603 0.02916±0.06329, p=0.649 for G5C2) (Figure 6C). Additionally, we observed no
604 significant difference in the density of stubby and mushroom spines between the
605 Control RNAi group and the Gas5 RNAi individuals (Stubby: 0.0029± 0.034, p= 0.931
606 for G5C1 and 0.0533±0.034, p= 0.138 for G5C2; Mushroom: 0.0232±0.0171, p=
607 0.1869 for G5C1 and 0.0265±0.0177, p= 0.1504 for G5C2) (Figure 6D-E).

608

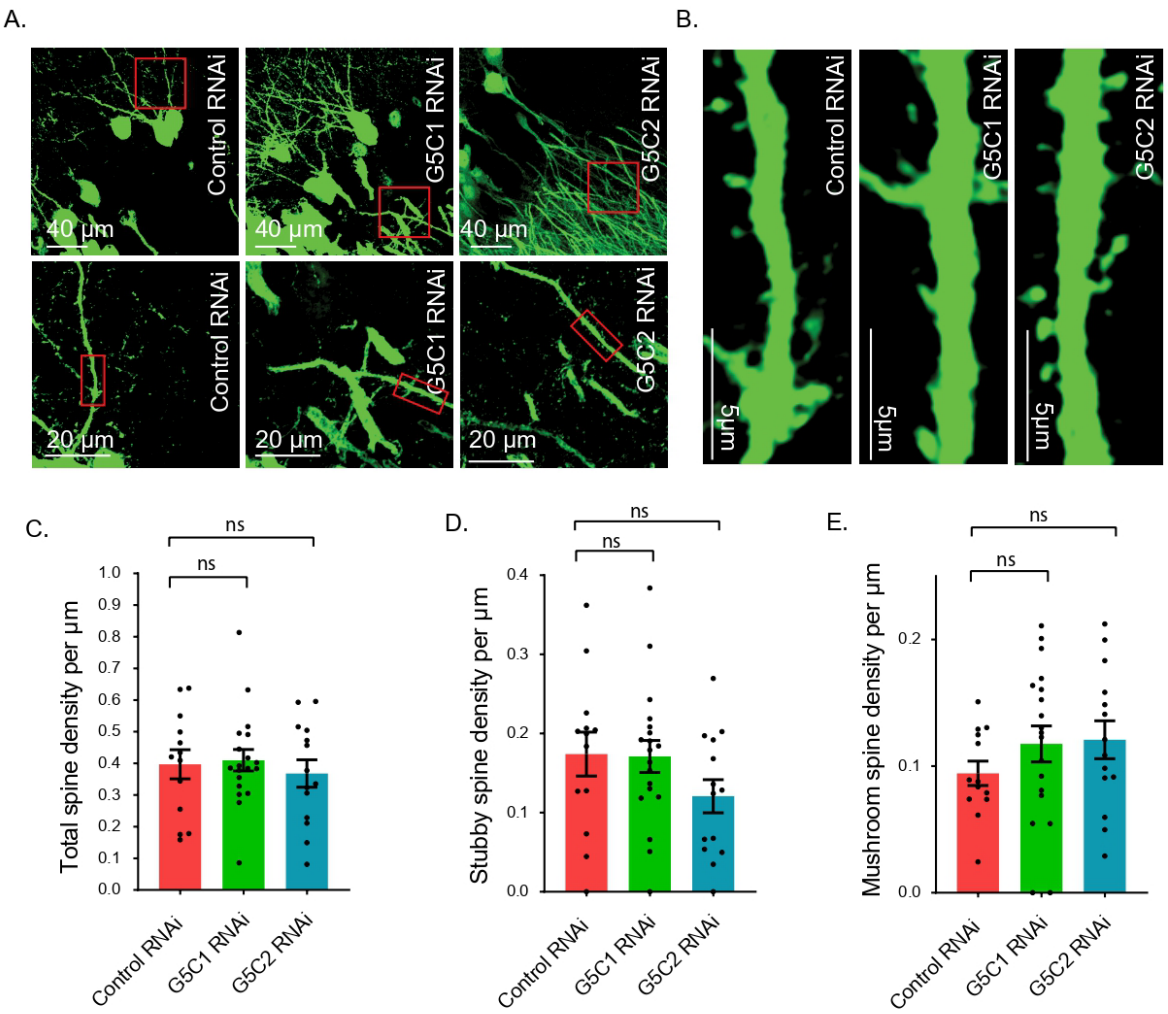

Figure 6. **Effect of Gas5 knockdown on spine development. A, B.** High magnification images of AAV injected mouse brain sections showing EGFP expressing hippocampal neurons; Control RNAi, G5C1 RNAi and G5C2 RNAi (left to right) respectively. **B**. Synapse density in hippocampal neurons of P30 mice injected with AAV at P0; Control RNAi, G5C1 RNAi and G5C2 RNAi (left to right) respectively. Quantification of **D.** total spine density, **E.** stubby spine density and **F.** mushroom spine density per µm in Control RNAi (UC), Gas5 C1 (G5C1) or Gas5 C2 (G5C2) shRNA; N=1, n=1-2, *n'*=13-19, *p<0.05; Data shows mean±SEM. Unpaired t-test with Welch's correction.

The underlying data is also shared in https://figshare.com/articles/dataset/_b_Gas5_regulates_early_life_stress-induced_anxiety_and_spatial_memory_b_/26047969 .

DISCUSSION

LncRNAs emerged as key regulatory RNAs involved in diverse cognitive functions (Mercer, Dinger, and Mattick 2009) (Samaddar and Banerjee 2021) (Liau et al. 2021). A recent study from our laboratory identified a set of synapse-enriched lncRNAs from the hippocampus (Samaddar et al., 2023). This study highlighted the importance of one such synapse-enriched lncRNA, Gas5, which in early life stress, evoked behavioural deficits. We observed that early life stress of maternal separation induces the expression of Gas5 in the hippocampus of male mice (Figure 1B). The reduction of Gas5 expression by RNAi alleviates MS-induced anxiety and rescues memory deficits (Figure 3–4). Apart from Gas5, maternal separation also induces the expression of another synapse-enriched lncRNA, Pantr1 (Figure 1B). The hippocampi of female pups (P21) were collected similarly to the male pups. The screen revealed a very different regulation of lncRNAs in female pups upon MS revealing the sexually dimorphic outcomes due to stress. Further behavioural experiments were done in males only as female behaviour is evidenced to be influenced by the oestrous cycle (Figure 2).

The *in situ* hybridization (Allen Brain Atlas) data showed that Gas5 is expressed in the CA1, CA2, CA3 and DG of both the dorsal and the ventral hippocampus (R. S. Patel et al. 2023), whereas, Pantr1 expression is mainly restricted to the CA1 region of the dorsal hippocampus (Goff et al. 2015). Differential expression of other lncRNAs is also observed in different neuronal populations of the hippocampus (CA1, CA2, CA3 and DG). For example, GM9968 is a lncRNA that is enriched in the hippocampus. Its expression spans through CA1, CA3 and DG in both the ventral and dorsal hippocampus, with a higher expression, especially in the ventral hippocampus. Meanwhile, another hippocampus-enriched lncRNA GM13644 is equally expressed in the ventral and dorsal hippocampus but higher at the DG compared to the CA1-CA3 regions (Kadakkuzha et al., 2015). These subregions of the hippocampus have been shown to have different functions (Tsien et al., 1996, Hitti and Siegelbaum, 2014, Nakashiba et al., 2008) and can also play a unique role in regulating the behaviour of an individual (Cui et al., 2022, Grinman et al., 2019, Butler et al., 2019). Existing literature shows that the dorsal hippocampus is involved in spatial memory formation (Moser and Moser 1998) and the ventral hippocampus has a prominent role in anxiety

(Fanselow and Dong 2010). Therefore, to probe the lncRNA function in MS-induced anxiety and memory, we have focused on Gas5.

The Gas5 lncRNA is involved in aggression (Feldker et al. 2003) and novelty-induced behaviour (Xu et al. 2020). Consistent with these observations, our study demonstrates the involvement of Gas5 in MS-induced anxiety (Figure 3). The maternally separated mouse displays a significant reduction in exploring the displaced object in our spatial object recognition test, indicating deficits in memory upon early life stress (Figure 4). These memory deficits are partially rescued by the Gas5 knockdown (Figure 4). Our observation of impaired spatial learning following maternal separation is in agreement with previous findings (Huot et al. 2002)(Grace et al. 2009)(Hulshof et al. 2011). However, the impaired cognitive performance with accompanied enhancement in anxiety differs from other studies that demonstrated improved spatial learning along with elevated levels of anxiety following maternal separation (Suri et al. 2013) (McGrath, Records, and Rice 2008). This discrepancy could arise due to the use of different rodent strains and paradigms to test hippocampus-dependent memory. We speculate that heightened anxiety upon maternal separation could contribute to hyperactivity that may lead to the exploration of both the displaced as well as the non-displaced object in our memory test (Figure 4). Our data shows that there is no bias between home-caged and maternally separated mice in their preference towards any object. Also, no preferential bias for any object is observed between mice expressing Gas5 shRNA or non-targeting control (Figure 4).

The role of direct Gas5 in hippocampus development is yet to be evaluated *in vivo,* although previous studies have shown that Gas5 has different expression patterns in young and old mice (Verbitsky et al., 2004). Aged mice showed a higher expression of Gas5. This finding was later supported by the fact that Alzheimer's disease AD patients had an elevated level of Gas5 in their hippocampus accompanied by a decrease in hippocampal volume (Chen et al., 2022). The molecular mechanism of regulation of Gas5 in the development of the hippocampus is still unexplored. A study done in Mouse Embryonic Hippocampal Progenitor cells showed an elevated Gas5 level accompanies neuronal commitment, while Gas5 downregulation occurs during terminal differentiation, suggesting a regulatory role in conjunction with connexin expression during neurogenesis (Rozental et al., 2000).

688 It is important to note that the Gas5 RNAi alone does not influence anxiety or memory
689 without any exposure to early life stress (Figure 3-4). This observation indicates that
690 the MS-induced Gas5 level above the physiological set point is a prerequisite for
691 anxiety and memory deficits due to early life stress. To evaluate whether the reversal
692 of ES-induced anxiety and memory deficits occurs due to reduced level of Gas5 in the
693 adult or developing brain, we have measured spine density and type from the adult
694 hippocampus (P38 – P40) following shRNA-mediated knockdown of the transcript
695 during development (P0). The spine density and type upon Gas5 knockdown were
696 assessed as these parameters are key determinants of anxiety and memory (Melo et
697 al., 2020; Leuner and Shors, 2013; Restivo et al., 2009; Kasai et al., 2010). No
698 significant changes in the density of the total spine, stubby spine and mushroom spine
699 were detected in the dendrites of hippocampal neurons (P38 - 40) following Gas5
700 knocked down (P0) (Figure 6). This observation confirms that the Gas5 activity during
701 neuronal development does not influence the reversal of MS-induced anxiety and
702 spatial memory deficit. The use of two distinct shRNAs against Gas5 (Figure S1) for
703 all experiments eliminates the possibility of an off-target effect and consequent
704 artefactual behavioural rescue or developmental changes. Taken together, our study
705 highlights an RNA-centric approach that could potentially ameliorate the debilitating
706 effect of early life stress.

707 For future investigations, employing alteration of Gas5 at distinct developmental
708 stages (P7, P14, P21, P35, P50) would be an ideal choice to show the temporal
709 resolution of Gas5 activity and its implications in reversing ES-induced elevated level
710 of anxiety and memory deficit during adolescence. This region-specific knockdown of
711 Gas5 through stereotaxic surgery, targeting specific regions such as CA1, CA2, CA3,
712 and DG, could provide deeper insights into its function within the dorsal and ventral
713 hippocampus. This can unravel the intricate role of Gas5 in modulating behaviour
714 through tailored assays, shedding light on its potential therapeutic implications of
715 Gas5. Further investigation is required to dissect a detailed mechanistic view of
716 lncRNA-dependent reversal of elevated anxiety and memory deficit upon ES. To
717 further understand the role of Gas5 in development, we can use the *in utero*-
718 electroporation technique to knockdown Gas5 at the embryonic stage and thereafter
719 study the development of the different types of the neural circuit of the hippocampus
720 (i.e. Perforant pathway, Mossy fibre pathway, Schaffer collateral pathway etc.). To

721 further understand the effect of Gas5 on functional changes at the synapse, we can
722 study the changes in electrophysiological properties of neurons using the patch-clamp
723 technique. This can help in elucidating the role of Gas5 in shaping the synaptic
724 landscape of the hippocampus during crucial developmental periods.

725 To gain a plausible mechanistic insight into the Gas5-mediated regulation of anxiety
726 and memory deficit upon maternal separation, we analyzed the functions of the Gas5
727 interacting transcripts identified from the POSTAR3 database. Our GO analysis
728 revealed that Gas5 interacting transcripts are involved in RNA metabolism and
729 synaptic functions. We have noted the regulation of transcripts associated with
730 translation, RISC loading complex, miRNA transport and RNA splicing. The GO
731 analysis also detected regulation of transcripts encoding proteins necessary for
732 dendritic transport of ribonucleoprotein complex, somatodendritic compartment and
733 ionotropic glutamate receptor binding. These observations impinge on the fact that
734 Gas5 could, potentially, regulate synaptic function *via* post-transcriptional regulation of
735 gene expression within subcellular spaces upon exposure to early life stress. Our data
736 shows that the expression of Argonaute, a component necessary for miRISC loading
737 and miRNA function, is reduced following the knockdown of Gas5. Consistent with
738 previous observations showing the involvement of miRNAs in early life stress-induced
739 gene expression (Allen and Dwivedi 2020), we speculate that Gas5-mediated
740 regulation of anxiety and memory upon maternal separation involves components of
741 the miRNA pathway. The enhanced expression of Argonaute may shift the miRNA
742 loading between coding transcript and Gas5 *via* promoting molecular decoy activity to
743 alter the translation status (Eulalio, Huntzinger, and Izaurralde 2008) (J. Li, Lv, and
744 Che 2020). In our investigation, we identified six transcripts modulated by Gas5 (Fus,
745 Hnrnph1, Hnrnpa2b1, Hnrnph2, Cpeb4 and Pcbp1), all pivotal in synaptic activity,
746 using existing CLIP-seq data from the POSTAR3 database. Concurrently, other
747 studies have focused on Gas5-mediated molecular framework regulating RNA
748 processing operating in the infralimbic cortex for fear-memory extinction (Liau et al.,
749 2023). The study proposes an interaction of Gas5 with Capirin1 (Cell Cycle Regulated
750 Protein 1) and G3BP2 (Stress Granule Assembly Factor 2) at the synapse during fear
751 extinction learning. The interaction of Gas5 with these RNA-granule proteins leads to
752 the sequestering of Capirini and G3BP2 at the synapse. Caprin1 is evidenced to be
753 important for the transport and translation of proteins essential for synaptic functions

754 (Pavinato et al., 2023) and G3BP2 helps in RNA localization and stabilization (Jin et
755 al., 2022). Therefore, sequestering of Caprin1 and G3BP2 alters synaptic plasticity
756 through local translation of proteins. A separate study exploring Gas5's role in
757 addiction enlisted its targets in the nucleus accumbens (NcA), uncovering 16,053
758 potential interactors (Xu et al., 2020). Our comparative analysis revealed an overlap
759 of 354 Gas5 targets between the NcA and hippocampus datasets, hinting at shared
760 regulatory mechanisms across distinct brain regions.

761 We have performed a KEGG pathway and Gene Ontology analysis to determine the
762 functional activities of these interacting partners of Gas5. The GO analysis revealed
763 that Gas5 is predominantly involved in the regulation of RNA processing and
764 translation of transcripts encoding proteins influencing synaptic function through the
765 regulation of biological processes (pre and postsynaptic endocytosis, stress granule
766 assembly, dendritic spine morphogenesis, regulation of axon extension, neuronal
767 differentiation etc.), cellular components (polysome, growth cone, synapse, neuron
768 projection etc.), and molecular functions (dopamine receptor binding, glutamate
769 receptor binding, mRNA binding, GTPase activity etc.). KEGG pathway analysis
770 indicated the involvement of Gas5 in key signalling pathways, c e.g. cAMP, mTOR and
771 Wnt, that regulate synaptic functions in developing and adult brains (Ma et al., 2022,
772 Grinman et al., 2021, Chen *et al.*, 2020). These pathways have been shown to directly
773 influence anxiety and memory (Gafford et al., 2013, Zhang et al., 2011, Moore and
774 Loprinzi, 2021, Wang et al., 2020, Argyrousi et al., 2020, Bertagna et al., 2021) (Figure
775 7) For details see Table S2 and Supplementary data).

776

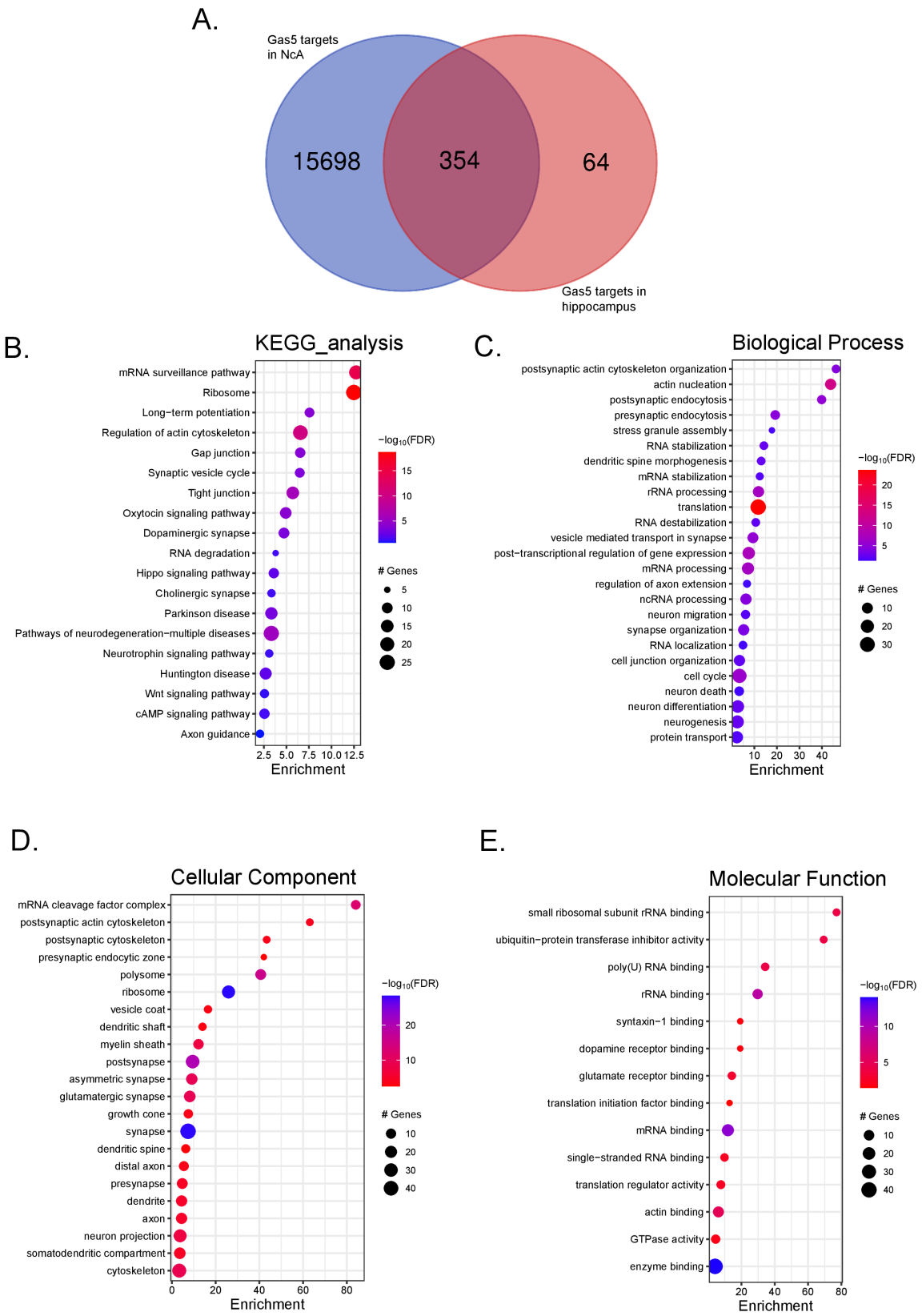
A.
Gas5 targets in NcA
15698
354
64
Gas5 targets in hippocampus
B.
KEGG_analysis
mRNA surveillance pathway
Ribosome
Long−term potentiation
Regulation of actin cytoskeleton
Gap junction
Synaptic vesicle cycle
Tight junction
Oxytocin signaling pathway
Dopaminergic synapse
RNA degradation
Hippo signaling pathway
Cholinergic synapse
Parkinson disease
Pathways of neurodegeneration−multiple diseases
Neurotrophin signaling pathway
Huntington disease
Wnt signaling pathway
cAMP signaling pathway
Axon guidance
2.5 5.0 7.5 10.0 12.5
Enrichment
−log10(FDR)
15
10
5
Genes
5
10
15
20
25
C.
Biological Process
postsynaptic actin cytoskeleton organization
actin nucleation
postsynaptic endocytosis
presynaptic endocytosis
stress granule assembly
RNA stabilization
dendritic spine morphogenesis
mRNA stabilization
rRNA processing
translation
RNA destabilization
vesicle mediated transport in synapse
post−transcriptional regulation of gene expression
mRNA processing
regulation of axon extension
ncRNA processing
neuron migration
synapse organization
RNA localization
cell junction organization
cell cycle
neuron death
neuron differentiation
neurogenesis
protein transport
10 20 30 40
Enrichment
−log10(FDR)
20
15
10
5
Genes
10
20
30
D.
Cellular Component
mRNA cleavage factor complex
postsynaptic actin cytoskeleton
postsynaptic cytoskeleton
presynaptic endocytic zone
polysome
ribosome
vesicle coat
dendritic shaft
myelin sheath
postsynapse
asymmetric synapse
glutamatergic synapse
growth cone
synapse
dendritic spine
distal axon
presynapse
dendrite
axon
neuron projection
somatodendritic compartment
cytoskeleton
0 20 40 60 80
Enrichment
−log10(FDR)
20
10
Genes
10
20
30
40
E.
Molecular Function
small ribosomal subunit rRNA binding
ubiquitin−protein transferase inhibitor activity
poly(U) RNA binding
rRNA binding
syntaxin−1 binding
dopamine receptor binding
glutamate receptor binding
translation initiation factor binding
mRNA binding
single−stranded RNA binding
translation regulator activity
actin binding
GTPase activity
enzyme binding
20 40 60 80
Enrichment
−log10(FDR)
10
5
Genes
10
20
30
40

779 **Figure 7**. **Gas5 targets are involved in the modulation of synapse and translation in the**
780 **nucleus accumbens and the hippocampus. A**. An overlap of the number of Gas5 targeted
781 coding transcripts regulating addiction in the nucleus accumbens (NcA) (Xu et al. 2020) and
782 fear memory extinction in the hippocampus (Liau et al. 2023). Gas5 interacting coding
783 transcripts were used to analyse their involvement in the **B**. KEGG pathway and Enrichment
784 pathways in Gene Ontology analysis of **C**. Biological processes, **D**. Cellular components, and
785 **E.** Molecular functions. FDR<0.05.

786 The underlying data is also shared in
787 https://figshare.com/articles/dataset/_b_Gas5_regulates_early_life_stress-
788 induced_anxiety_and_spatial_memory_b_/26047969 .

789

790

791 In our study, the knockdown of synapse-enriched transcripts of Gas5 could lead to the
792 sequestering of RNA-binding proteins (RBPs), disrupting translation dynamics at
793 these neuronal junctions. The Gas5 transcript's interaction with RBPs might influence
794 how these proteins are compartmentalized within distinct synaptic subcellular spaces.
795 This reorganization could restrict RBPs' access to other mRNAs, causing shifts in local
796 protein synthesis at the synapse and ultimately impacting synaptic plasticity.

797 Gas5 immunoprecipitation, coupled with Mass spectrometry analysis from
798 hippocampal tissue of stressed animals, holds promise for uncovering novel protein
799 candidates and pathways. By examining the varied expression of Gas5 targets,
800 manipulating their levels via overexpression or loss of function can offer critical insights
801 into the potential reversibility of early-life stress impacts. Leveraging CRISPR-Cas-
802 inspired RNA targeting systems (CIRTs), Gas5 targets can be precisely targeted at
803 the synapse, shedding light on their role in synapse development and plasticity.
804 Additionally, it can also be used to rescue stress-induced anxiety and loss of memory
805 offering a scope for therapeutic intervention.

806

807 The use of CO_2 gas for euthanasia might be considered a limitation of our study as the
808 high level of CO2 may trigger the expression of early-effect gene cFos and can also

affect other gene expressions due to a panic attack at the moment of euthanasia (Johnson et al., 2011, Khokhlova et al., 2022). However, maternal separation data is normalised as the ratio between homecaged control and maternally separated animals. Hence, the probable artefact due to the euthanasia method is significantly minimized.

Overall, our study highlights the importance of evaluating diverse lncRNA activities during early life stress. To gain mechanistic insight, it would be important to understand how lncRNA activity is modulated by early life stress and its consequence on cognitive performance. We believe that this study will promote further research to probe how early life stress across temporal windows could lead to behavioural diversity *via* non-coding RNA-mediated regulation of gene expression.

AUTHOR CONTRIBUTION

D.B. and S.B. conceptualized the project. D.B. performed all experiments. S.S. performed spatial memory and anxiety analysis. D.B. and S.B. wrote the manuscript.

ACKNOWLEDGEMENT

We thank Penn Vector Core for AAV vectors. We acknowledge Balakumar Srinivasan for GO analysis, Gourav Sharma for spatial memory set-up, Smruti Mhalgi for blind scoring of SOR data, Kamakshi Garg for assisting in confocal microscopy and Sarbani Samaddar for conceptual discussions and proofreading of this manuscript. This work is supported by extramural research grant BT/PR14071/GET/119/36/2015 (to S.B.) from the Department of Biotechnology, Government of India and the core fund of the National Brain Research Centre.

All art has been created with BioRender.com (Figure 1-4, S 1A-B, S 5 and Graphical Abstract).

CONFLICTS OF INTEREST

The authors declare no conflict of interest.

DATA AVAILABILITY

The data supporting this study's findings are available at https://figshare.com/articles/dataset/_b_Gas5_regulates_early_life_stress-induced_anxiety_and_spatial_memory_b_/26047969. Additionally, a preprint of the manuscript is available on Biorxiv https://www.biorxiv.org/content/biorxiv/early/2023/09/27/2023.09.27.559778.full.pdf posted on 27th of September 2023.

REFERENCES

Allen, Lauren, and Yogesh Dwivedi. 2020. "MicroRNA Mediators of Early Life Stress Vulnerability to Depression and Suicidal Behavior." *Molecular Psychiatry* 25(2): 308–20. http://dx.doi.org/10.1038/s41380-019-0597-8.

Balouek, Julie-anne et al. 2023. "Reactivation of Early-Life Stress-Sensitive Neuronal Ensembles Contributes to Lifelong Stress Hypersensitivity." 43(34): 5996–6009.

Bannerman, David M. et al. 2014. "Hippocampal Synaptic Plasticity, Spatial Memory and Anxiety." *Nature Reviews Neuroscience* 15(3): 181–92.

Banqueri, María, Marta Méndez, and Jorge L. Arias. 2017. "Behavioral Effects in Adolescence and Early Adulthood in Two Length Models of Maternal Separation in Male Rats." *Behavioural Brain Research* 324: 77–86. http://dx.doi.org/10.1016/j.bbr.2017.02.006.

Barkus, Christopher et al. 2010. "Hippocampal NMDA Receptors and Anxiety: At the Interface between Cognition and Emotion." *European Journal of Pharmacology* 626(1): 49–56. http://dx.doi.org/10.1016/j.ejphar.2009.10.014.

Blum, Sonja, Anthony N. Moore, Frank Adams, and Pramod K. Dash. 1999. "A Mitogen-Activated Protein Kinase Cascade in the CA1/CA2 Subfield of the Dorsal Hippocampus Is Essential for Long-Term Spatial Memory." *Journal of Neuroscience* 19(9): 3535–44.

Bourin, Michel, and Martine Hascoët. 2003. "The Mouse Light/Dark Box Test." *European Journal of Pharmacology* 463(1–3): 55–65.

865 Christensen, Mette, Lars A. Larsen, Sakari Kauppinen, and Gerhard Schratt. 2010.
866 "Recombinant Adeno-Associated Virus-Mediated MicroRNA Delivery into the Postnatal
867 Mouse Brain Reveals a Role for MiR-134 in Dendritogenesis in Vivo." *Frontiers in*
868 *Neural Circuits* 3(JAN): 1–10.

869 Cui, Xiaoli et al. 2022. "Identification and Characterization of Long Non-Coding RNA Carip in
870 Modulating Spatial Learning and Memory." *Cell Reports* 38(8): 110398.
871 https://doi.org/10.1016/j.celrep.2022.110398.

872 Daniels, W. M.U., C. Y. Pietersen, M. E. Carstens, and D. J. Stein. 2004. "Maternal
873 Separation in Rats Leads to Anxiety-like Behavior and a Blunted ACTH Response and
874 Altered Neurotransmitter Levels in Response to a Subsequent Stressor." *Metabolic*
875 *Brain Disease* 19(1–2): 3–14.

876 Denninger, Jiyeon K., Bryon M. Smith, and Elizabeth D. Kirby. 2018. "Novel Object
877 Recognition and Object Location Behavioral Testing in Mice on a Budget." *Journal of*
878 *Visualized Experiments* 2018(141): 1–10.

879 Dimatelis, J. J., V. A. Russell, D. J. Stein, and W. M. Daniels. 2014. "Methamphetamine
880 Reversed Maternal Separation-Induced Decrease in Nerve Growth Factor in the Ventral
881 Hippocampus." *Metabolic Brain Disease* 29(2): 433–39.

882 Eulalio, Ana, Eric Huntzinger, and Elisa Izaurralde. 2008. "GW182 Interaction with
883 Argonaute Is Essential for MiRNA-Mediated Translational Repression and MRNA
884 Decay." *Nature Structural and Molecular Biology* 15(4): 346–53.

885 Fanselow, Michael S., and Hong Wei Dong. 2010. "Are the Dorsal and Ventral Hippocampus
886 Functionally Distinct Structures?" *Neuron* 65(1): 7–19.
887 http://dx.doi.org/10.1016/j.neuron.2009.11.031.

888 Feldker, Dorine E.M. et al. 2003. "GeneChip Analysis of Hippocampal Gene Expression
889 Profiles of Short- and Long-Attack-Latency Mice: Technical and Biological Implications."
890 *Journal of Neuroscience Research* 74(5): 701–16.

891 File, Sandra E., Paul J. Kenny, and Survjit Cheeta. 2000. "The Role of the Dorsal
892 Hippocampal Serotonergic and Cholinergic Systems in the Modulation of Anxiety."
893 *Pharmacology Biochemistry and Behavior* 66(1): 65–72.

894 Goff, Loyal A. et al. 2015. "Spatiotemporal Expression and Transcriptional Perturbations by

895 Long Noncoding RNAs in the Mouse Brain." *Proceedings of the National Academy of*
896 *Sciences of the United States of America* 112(22): 6855–62.

897 Grace, Laurian et al. 2009. "Effect of Exercise on Learning and Memory in a Rat Model of
898 Developmental Stress." *Metabolic Brain Disease* 24(4): 643–57.

899 Hu, Boqin et al. 2017. "POSTAR: A Platform for Exploring Post-Transcriptional Regulation
900 Coordinated by RNA-Binding Proteins." *Nucleic Acids Research* 45(D1): D104–14.

901 Hulshof, Henriëtte J. et al. 2011. "Maternal Separation Decreases Adult Hippocampal Cell
902 Proliferation and Impairs Cognitive Performance but Has Little Effect on Stress
903 Sensitivity and Anxiety in Adult Wistar Rats." *Behavioural Brain Research* 216(2): 552–
904 60.

905 Huot, Rebecca L., Paul M. Plotsky, Robert H. Lenox, and Robert K. McNamara. 2002.
906 "Neonatal Maternal Separation Reduces Hippocampal Mossy Fiber Density in Adult
907 Long Evans Rats." *Brain Research* 950(1–2): 52–63.

908 Izquierdo, Ivan, and Jorge H. Medina. 1997. "Memory Formation: The Sequence of
909 Biochemical Events in the Hippocampus and Its Connection to Activity in Other Brain
910 Structures." *Neurobiology of Learning and Memory* 68(3): 285–316.

911 Jimenez, Jessica C. et al. 2018. "Anxiety Cells in a Hippocampal-Hypothalamic Circuit."
912 *Neuron* 97(3): 670-683.e6.

913 Kaech, Stefanie, and Gary Banker. 2006. "Culturing Hippocampal Neurons." *Nature*
914 *Protocols* 1(5): 2406–15.

915 Kalisch, Raffael et al. 2006. "Anxiety and Hippocampus Volume in the Rat."
916 *Neuropsychopharmacology* 31(5): 925–32.

917 Kasai, Haruo et al. 2010. "Structural Dynamics of Dendritic Spines in Memory and
918 Cognition." *Trends in Neurosciences* 33(3): 121–29.
919 http://dx.doi.org/10.1016/j.tins.2010.01.001.

920 Katsouli, S. et al. 2014. "Sexually Dimorphic Long-Term Effects of an Early Life Experience
921 on AMPA Receptor Subunit Expression in Rat Brain." *Neuroscience* 257: 49–64.
922 http://dx.doi.org/10.1016/j.neuroscience.2013.10.073.

Kim, Ji Yoen et al. 2014. “Intracerebroventricular Viral Injection of the Neonatal Mouse Brain for Persistent and Widespread Neuronal Transduction.” *Journal of Visualized Experiments* (91): 1–7.

Korosi, A. et al. 2012. “Early-Life Stress Mediated Modulation of Adult Neurogenesis and Behavior.” *Behavioural Brain Research* 227(2): 400–409. http://dx.doi.org/10.1016/j.bbr.2011.07.037.

Kremmyda, Olympia et al. 2016. “Beyond Dizziness: Virtual Navigation, Spatial Anxiety and Hippocampal Volumein Bilateral Vestibulopathy.” *Frontiers in Human Neuroscience* 10(MAR2016): 1–12.

Leger, Marianne et al. 2013. “Object Recognition Test in Mice.” *Nature Protocols* 8(12): 2531–37.

Leuner, B., and T. J. Shors. 2013. “Stress, Anxiety, and Dendritic Spines: What Are the Connections?” *Neuroscience* 251: 108–19. http://dx.doi.org/10.1016/j.neuroscience.2012.04.021.

Li, Hongzhu et al. 2022. “Loss of SST and PV Positive Interneurons in the Ventral Hippocampus Results in Anxiety-like Behavior in 5xFAD Mice.” *Neurobiology of Aging* 117: 165–78. https://doi.org/10.1016/j.neurobiolaging.2022.05.013.

Li, Jie, Hui Lv, and Yu Qin Che. 2020. “Long Non-Coding RNA Gas5 Potentiates the Effects of MicroRNA-21 Downregulation in Response to Ischaemic Brain Injury.” *Neuroscience* 437: 87–97. https://doi.org/10.1016/j.neuroscience.2020.01.014.

Liau, Wei Siang et al. 2023. “Fear Extinction Is Regulated by the Activity of Long Noncoding RNAs at the Synapse.” *Nature Communications* 14(1).

Liau, Wei Siang, Sarbani Samaddar, Sourav Banerjee, and Timothy W. Bredy. 2021. “On the Functional Relevance of Spatiotemporally-Specific Patterns of Experience-Dependent Long Noncoding RNA Expression in the Brain.” *RNA Biology* 18(7): 1025–36. https://doi.org/10.1080/15476286.2020.1868165.

Lundberg, Stina, Ingrid Nylander, and Erika Roman. 2020. “Behavioral Profiling in Early Adolescence and Early Adulthood of Male Wistar Rats After Short and Prolonged Maternal Separation.” *Frontiers in Behavioral Neuroscience* 14(March): 1–10.

Marais, Lelanie, Suzél M. Hattingh, Dan J. Stein, and Willie M.U. Daniels. 2009. “A Proteomic Analysis of the Ventral Hippocampus of Rats Subjected to Maternal Separation and Escitalopram Treatment.” *Metabolic Brain Disease* 24(4): 569–86.

Mattick, John S. et al. 2023. “Long Non-Coding RNAs: Definitions, Functions, Challenges and Recommendations.” *Nature Reviews Molecular Cell Biology* 24(June): 430–47.

McGrath, J. M., K. Records, and M. Rice. 2008. “基因的改变NIH Public Access.” *Infant behavior and development* 31(1): 71–80.

Mckibben, Lauren A., and Yogesh Dwivedi. 2021. “Early-Life Stress Induces Genome-Wide Sex-Dependent MiRNA Expression and Correlation across Limbic Brain Areas in Rats.” *Epigenomics* 13(13): 1031–56.

McNaughton, Neil. 1997. “Cognitive Dysfunction Resulting from Hippocampal Hyperactivity - A Possible Cause of Anxiety Disorder?” *Pharmacology Biochemistry and Behavior* 56(4): 603–11.

Melo, Silvana Regina de, Caren Tatiane de David Antoniazzi, Shakhawat Hossain, and Bryan Kolb. 2020. “Short Predictable Stress Promotes Resistance to Anxiety Behavior and Increases Dendritic Spines in Prefrontal Cortex and Hippocampus.” *Brain Research* 1746(July): 147020. https://doi.org/10.1016/j.brainres.2020.147020.

Mercer, Tim R., Marcel E. Dinger, and John S. Mattick. 2009. “Long Non-Coding RNAs: Insights into Functions.” *Nature Reviews Genetics*.

Monroy, Elibeth, Elizabeth Hernández-Torres, and Gonzalo Flores. 2010. “Maternal Separation Disrupts Dendritic Morphology of Neurons in Prefrontal Cortex, Hippocampus, and Nucleus Accumbens in Male Rat Offspring.” *Journal of Chemical Neuroanatomy* 40(2): 93–101.

Morris, Richard G.M. et al. 2006. “Memory Reconsolidation: Sensitivity of Spatial Memory to Inhibition of Protein Synthesis in Dorsal Hippocampus during Encoding and Retrieval.” *Neuron* 50(3): 479–89.

Moser, May Britt, and Edvard I. Moser. 1998. “Functional Differentiation in the Hippocampus.” *Hippocampus* 8(6): 608–19.

980 Patel, Rekha S. et al. 2023. “Small Molecule Targeting Long Noncoding RNA GAS5
981 Administered Intranasally Improves Neuronal Insulin Signaling and Decreases
982 Neuroinflammation in an Aged Mouse Model.” *Scientific Reports* 13(1): 1–18.
983 https://doi.org/10.1038/s41598-022-27126-6.

984 Patel, Tapan P. et al. 2014. “An Open-Source Toolbox for Automated Phenotyping of Mice in
985 Behavioral Tasks.” *Frontiers in Behavioral Neuroscience* 8(OCT): 1–16.

986 Pickering, Chris et al. 2006. “Repeated Maternal Separation of Male Wistar Rats Alters
987 Glutamate Receptor Expression in the Hippocampus but Not the Prefrontal Cortex.”
988 *Brain Research* 1099(1): 101–8.

989 Restivo, Leonardo, Gisella Vetere, Bruno Bontempi, and Martine Ammassari-Teule. 2009.
990 “The Formation of Recent and Remote Memory Is Associated with Time-Dependent
991 Formation of Dendritic Spines in the Hippocampus and Anterior Cingulate Cortex.”
992 *Journal of Neuroscience* 29(25): 8206–14.

993 Revest, J. M. et al. 2009. “Adult Hippocampal Neurogenesis Is Involved in Anxiety-Related
994 Behaviors.” *Molecular Psychiatry* 14(10): 959–67.

995 Rodriguez, Alvaro et al. 2018. “ToxTrac: A Fast and Robust Software for Tracking
996 Organisms.” *Methods in Ecology and Evolution* 9(3): 460–64.

997 Samaddar Sarbani. 2023. “Transcriptomic Analysis Identifies Synapse-Enriched LncRNAs
998 Required for Excitatory Synapse Development and Fear Memory.” *bioRxiv*: 1–50.
999 https://www.biorxiv.org/content/10.1101/2023.07.14.549055v2.full.pdf.

1000 Samaddar, Sarbani, and Sourav Banerjee. 2021. “Far from the Nuclear Crowd: Cytoplasmic
1001 LncRNA and Their Implications in Synaptic Plasticity and Memory.” *Neurobiology of*
1002 *Learning and Memory* 185(April): 107522. https://doi.org/10.1016/j.nlm.2021.107522.

1003 Shi, Changhua, Ling Zhang, and Chuan Qin. 2017. “Long Non-Coding RNAs in Brain
1004 Development, Synaptic Biology, and Alzheimer’s Disease.” *Brain Research Bulletin*
1005 132(5): 160–69. http://dx.doi.org/10.1016/j.brainresbull.2017.03.010.

1006 Sood, Ankit et al. 2018. “Early Emergence of Altered 5-HT2A Receptor-Evoked Behavior,
1007 Neural Activation and Gene Expression Following Maternal Separation.” *International*
1008 *Journal of Developmental Neuroscience* 65(May 2017): 21–28.
1009 https://doi.org/10.1016/j.ijdevneu.2017.10.005.

1010 Soutschek, Michael, and Gerhard Schratt. 2023. “Non-Coding RNA in the Wiring and
1011 Remodeling of Neural Circuits.” *Neuron*: 1–15.
1012 http://www.ncbi.nlm.nih.gov/pubmed/37230080.

1013 Spadaro, Paola A. et al. 2015. “Long Noncoding RNA-Directed Epigenetic Regulation of
1014 Gene Expression Is Associated with Anxiety-like Behavior in Mice.” *Biological*
1015 *Psychiatry* 78(12): 848–59. http://dx.doi.org/10.1016/j.biopsych.2015.02.004.

1016 Sterley, Toni Lee, Fleur M. Howells, and Vivienne A. Russell. 2013. “Maternal Separation
1017 Increases GABAA Receptor-Mediated Modulation of Norepinephrine Release in the
1018 Hippocampus of a Rat Model of ADHD, the Spontaneously Hypertensive Rat.” *Brain*
1019 *Research* 1497: 23–31. http://dx.doi.org/10.1016/j.brainres.2012.12.029.

1020 Suri, Deepika et al. 2013. “Early Stress Evokes Age-Dependent Biphasic Changes in
1021 Hippocampal Neurogenesis, Bdnf Expression, and Cognition.” *Biological Psychiatry*
1022 73(7): 658–66. http://dx.doi.org/10.1016/j.biopsych.2012.10.023.

1023 Takao, Keizo, and Tsuyoshi Miyakawa. 2006. “Light/Dark Transition Test for Mice.” *Journal*
1024 *of Visualized Experiments* (1): 1–3.

1025 Tang, Doudou et al. 2023. “SRplot: A Free Online Platform for Data Visualization and
1026 Graphing.” *PLoS ONE* 18(11 October): 1–8.
1027 http://dx.doi.org/10.1371/journal.pone.0294236.

1028 Taylor, Shelley E. 2010. “Mechanisms Linking Early Life Stress to Adult Health Outcomes.”
1029 *Proceedings of the National Academy of Sciences of the United States of America*
1030 107(19): 8507–12.

1031 Wang, Andi, Junbao Wang, Ying Liu, and Yan Zhou. 2017. “Mechanisms of Long Non-
1032 Coding RNAs in the Assembly and Plasticity of Neural Circuitry.” *Frontiers in Neural*
1033 *Circuits* 11(October).

1034 Wang, Xiaobing et al. 2022. “Maternal Separation Affects Anxiety-like Behavior Beginning in
1035 Adolescence and Continuing through Adulthood and Related to Dnmt3a Expression.”
1036 *Journal of Neurophysiology* 128(3): 611–18.

1037 Wimmer, Mathieu E., Pepe J. Hernandez, Jennifer Blackwell, and Ted Abel. 2012. “Aging
1038 Impairs Hippocampus-Dependent Long-Term Memory for Object Location in Mice.”
1039 *Neurobiology of Aging* 33(9): 2220–24.

1040 http://dx.doi.org/10.1016/j.neurobiolaging.2011.07.007.

1041 Xu, Haiyang et al. 2020. “Role of Long Noncoding RNA Gas5 in Cocaine Action.” *Biological*
1042 *Psychiatry* 88(10): 758–66. https://doi.org/10.1016/j.biopsych.2020.05.004.

1043 Zhang, Xuejing, Milton H. Hamblin, and Ke Jie Yin. 2017. “The Long Noncoding RNA
1044 Malat1: Its Physiological and Pathophysiological Functions.” *RNA Biology* 14(12):
1045 1705–14. https://doi.org/10.1080/15476286.2017.1358347.

1046